Stochastic self-oscillations and turbulence

M. I. Rabinovich

Institute of Applied Physics, Academy of Sciences of the USSR, Gor'kiĭ
Usp. Fiz. Nauk **125**, 123–168 (May 1978)

Until quite recently, it was thought that turbulence, i.e., stochastic self-oscillations of a continuous medium, was related exclusively to the excitation of an exceedingly large number of degrees of freedom. This review is devoted to the discussion of new ideas on the nature of the unpredictable turbulent motions in dissipative media connected with the discovery of strange attractors, i.e., attractive regions in phase space within which all paths are unstable and behave in a very complex fashion (motions on an attractor of this kind are characterized by a continuous spectrum). Turbulence represented by a strange attractor is described by a finite number of degrees of freedom, i.e., modes whose physical nature may be different. The example of a simple electronic noise generator is used to illustrate how the instability (divergence) of such paths leads to stochastic behavior. The analysis is based on the introduction of a nonreciprocally single-valued Poincaré mapping onto itself, which is then used to describe the strange attractors encountered in different physical problems. An example of this mapping is used to demonstrate the discrete, symbolic, description of dynamic systems. The properties of such systems which indicate their stochastic nature, for example, positive topologic entropy and hyperbolicity are discussed. Specific physical mechanisms leading to the appearance of stochastic behavior and characterized by a continuous time spectrum are discussed. Strange attractors that appear in the case of parametric instability of waves in plasmas, laser locking by an external field, and so on, are demonstrated. "Attractor models" of hydrodynamic turbulence are reviewed, and in particular, finite-dimensional hydrodynamic models of convection in a layer and of Couette flow between rotating cylinders are constructed and found to exhibit stochastic behavior.

PACS numbers: 47.25. – c, 02.50.Ey

CONTENTS

INTRODUCTION

The problem of turbulence arose in the middle of the last century when many apparently irreconcilable contradictions appeared between theoretical hydrodynamics (with its Navier-Stokes equations) and applied problems on the flow of a liquid or gas. For example, it was known to the experimenters that, for sufficiently high flow velocities of a liquid in a pipe, the resistance to flow increases as the square of the average (over the cross section) velocity. This is the Chezy law. On the other hand, theory shows that this resistance should increase in proportion to the first power of the velocity, which is the Poiseuille law. The first step toward the reconciliation of these contradictions was made by Osborn Reynolds, who published in 1883 a

 0038-5670/78/050443-26$01.10

paper describing experiments with colored streamers injected into a flow of fluid, in which he introduced his celebrated number $\mathrm{Re}=vD/\nu$ (D is the diameter, v the velocity, and ν the kinematic viscosity) and, for the first time, related Poiseuille's law to the layered, laminar, flow of a liquid and Chezy's law to the irregular, random, turbulent motion. He established that laminar motion was stable only for $\mathrm{Re}<2000$ and that turbulence set in for higher values of Re. Thus, for water flowing in a tube with a diameter of 1 cm at room temperature, the laminar state "ends," as a rule, at average flow velocities $\leqslant 30$ cm/sec.

The problem of turbulence, which thus arose almost a hundred years ago, and involves the elucidation of the nature of the random motion of a nonlinear medium and the development of methods for its self-consistent description, has remained to this day one of the most attractive and intriguing problems in classical physics, and is still a long way from its final solution.[1)] The problem of turbulence, which originally appeared in hydrodynamics, is, in fact, common to plasma physics, cosmology, ecology, weather forecasting, the theory of planets and stars, chemical kinetics, radiophysics, and many other branches of science.

The central question in the problem of turbulence in all its physical and other manifestations has always been and still is the question of its nature, i.e., the reasons for and the mechanisms of generating disorder.

At different times, there were a number of models that attracted enthusiastic support and claimed to explain the mechanisms responsible for the appearance of turbulence in nonlinear dynamic systems but, each time, it was not long before their inadequacies were demonstrated. The Landau-Hopf model is the most lasting and describes the origin of turbulence in terms of a long chain of successive instabilities, the result of which is that the motion becomes very complicated and tortuous. Right now, we are in the midst of one of the recurring upturns in the history of the theory of turbulence, associated with the development of new ideas on the stochastic character of self-oscillating dynamic systems and the discovery of the so-called "*strange attractors*" by Edward Lorenz, Ruelle and Takens, Smale, and others.

In the same way that a limit cycle in the phase space of a dynamic system is a mapping of periodic self-oscillations (A. A. Andronov[2]), the attractive random set or, as it is usually called, *the strange attractor*, on which all the paths are unstable and behave in a complicated and tortuous fashion, is the mathematical mapping of *stochastic self-oscillations*. Stochastic self-oscillations and turbulence are intimately related. This was discussed by G. S. Gorelik as far back as the early 1950's: "*Turbulence*, with its limit of self-excitation, with the characteristic hysteresis in its appearance and disappearance as the velocity of the flow producing it is increased or reduced, and the primary role of nonlinearity in its developed (stationary) state, is, in fact, a *self-oscillation*. Its specific features are determined by the fact that it is a self-oscillation of a continuous medium, i.e., a system with an infinite number of degrees of freedom."[3]

The belief that the transition of a self-oscillatory system to the turbulent state requires the excitation of at least an exceedingly large (if not infinite) number of degrees of freedom is very widely held. This is, clearly, connected with the particular understanding of stochasticity of dynamic systems that has emerged in statistical mechanics: the motion of each individual particle in a gas is, in principle, known and predictable, but the motion of a system consisting of a very large number of particles (even noninteracting particles) is so complicated that its dynamic description loses all meaning (even though it is possible, in principle!). Moreover, not all the initial conditions are known absolutely accurately. Hence the need for the average statistical description. The self-oscillatory nature of the motion of the system (continuous medium) is essential, according to these ideas, only during the establishment of stationary pulsations, i.e., the balance between the supply of energy by the source (for example, the source of a flow) and dissipation determines the intensity of the "self-oscillatory modes." In a steady state, this "gas of self-oscillators" should not, it seems, differ from a perfect gas. Analogous ideas lie at the basis of the model of turbulence put forward by Landau in 1944[4,5] and independently in a somewhat different form by Hopf in 1948.[6]

As the Reynolds number increases, the Landau-Hopf model suggests that turbulence appears as a result of a chain of successive bifurcations that leads to a *quasiperiodic* motion $u(t)=F(\omega_1 t,\ldots,\omega_N t)$, where the function F has the period of 2π in each of its arguments, and the ω_i are N irrationally coupled frequencies. The first bifurcations in this chain are very simple: the initially stable state of equilibrium is transformed into an unstable state and, at the same time, a stable limit cycle appears in its neighborhood (this is the way in which ω_1 appears). The resulting periodic motion then loses its stability, and a two-dimensional formation appears in the neighborhood of the stable cycle that has vanished, namely, a torus whose winding frequency is unrelated to the main frequency (this is the origin of ω_2). This doubly periodic motion then becomes unstable and a three-dimensional torus is created (ω_3 appears), and so on. When N is large, the realization of this quasiperiodic process does, in fact, appear to be random. In particular, its self-correlation function falls rapidly (as $1/\sqrt{N}$) and the time to its next maximum (Poincaré recurrence period[9]) is $T\sim\exp(\alpha N)$, where $\alpha\sim 1$.[8]

The turbulence model in the form of a "gas" of self-oscillatory modes with incommensurable frequencies, which is natural from the standpoint of the commonly accepted ideas, is, nevertheless, only partially valid.

[1)] In Feynman's words, "... we cannot cope with this 'wet water' spraying out of a hose. This is the central problem which, come one fair day, we shall have to solve but, as yet, we don't know how."[1]

The point is that the inclusion of even a slight interaction between the "particles" of this gas may lead to the instability of the multifrequency quasiperiodic motion in which we are interested. The disruption of this motion, which is represented in phase space by a circuit on the torus that is not closed, may result in the appearance of a periodic motion—the *limit cycle*—and the "real" stochastic motion, i.e., the *strange attractor*. The fact that a small change in the parameters of a self-oscillatory system may result in a transition from a quasiperiodic motion of the system to a periodic motion has been known for some time and is, in fact, the widely known phenomenon of *synchronization*[2] (cf., Sec. 2). Yet the possibility of creating a strange attractor during the disruption of quasiperiodic motion, i.e., the possibility of establishing as a result of some particular one in a series of bifurcations of stochastic (!) motion characterized by a continuous spectrum in place of motion with a discrete spectrum, was proved only quite recently by Ruelle and Takens[10] (1971). In the example considered by them, the number of independent frequencies preceding the appearance of stochastic behavior was four, but the stochasticity represented by a strange attractor can appear even in self-oscillatory system with only one and a half degrees of freedom (three-dimensional phase space) and certainly in a system with a large number of excited modes. Thus, it is not at all essential for the transition of the self-oscillatory system to a stochastic or, as we shall say, a turbulent state[3] to involve a very large number of excited degrees of freedom.

This review is largely devoted to the turbulence mapped by the strange attractor. This turbulence is described by a finite number of degrees of freedom, or modes, and may have different physical origins. The structure of modes forming the basis for the turbulent motion may also be different. For example, in an incompressible liquid, the elementary excitation is often conveniently represented by a system of vortices so that we have vortex turbulence. In a gas, a plasma, or a solid, we have waves (not necessarily sinusoidal!). Stochastic self-oscillations in an ensemble of quasiharmonic waves form *weak wave turbulence*.[57] When the waves are essentially nonsinusoidal, the result is *strong turbulence*. An example of wave turbulence in hydrodynamics is provided by the wave motion on the surface of the sea (here, the modes are the surface waves).

We begin our review with a discussion of the possibility of random motion in self-oscillatory dynamic systems. Analysis of the equations describing a simple electronic noise generator is used to show how path instability leads to stochastic behavior. The discussion is based on a nonsingular-valued *Poincaré mapping* of a segment onto itself, which is then used to describe the strange attractors encountered in different physical problems. An example of such mapping is used to demonstrate the discrete, *symbolic* description of dynamic systems. This is followed by a discussion of the stochastic features of such systems, including, in particular, the positive nature of *topologic entropy* and *hyperbolicity*. Next, a discussion is given of the physical mechanisms leading to the appearance of stochasticity mapped by strange attractors. Whenever possible, a description is given of the topologic structure of these attractors and of the bifurcations preceding them. "Attractor models" of hydrodynamic turbulence form the subject of the last chapter in which particular attention is devoted not to the properties of the attractors but to the development of finite-dimensional hydrodynamic models in which attractors appear, and to the discussion of the validity of such models in the case of classical flow.

1. DISORDER IN SELF-OSCILLATORY SYSTEMS AND MATHEMATICAL CRITERIA FOR STOCHASTIC BEHAVIOR

When stochasticity of dynamic systems is discussed, the problem arises as to how is it that random behavior can appear in a system that is free from fluctuations and is described by deterministic equations. The existence and uniqueness theorem would seem to guarantee that a given system will exhibit unique behavior for given initial conditions. When the system has an exceedingly large number of degrees of freedom (e.g., a gas), the situation appears to be a little simpler: in principle, the system can be described dynamically, but the motion is so complicated that the problem becomes unrealistic and reduces in actual fact to the choice of some suitable hypothesis (for example, the *ergodic hypothesis*) enabling us to go over to an average description. The question then is—how does stochastic behavior become established in systems with a small number of degrees of freedom?

The answer lies in the *instability* of all, or almost all, solutions for the system! This idea was most clearly expressed by Krylov[11] and, later, by Max Born[12] in connection with the foundations of statistical physics and the problem of predictability in classical mechanics. In particular, the physically sensible concept of determinability introduced by Born is essentially that, because of the presence of fluctuations, each state is always determined to within a small, but always finite, uncertainty ε and is therefore specified not by a number but by a certain probability distribution, so that the problem in mechanics is to predict the distribution at time t on the basis of a known initial distribution. If a given solution is stable, i.e., if initial perturbations do not grow, then a later state is predictable, and the theory can be referred to as deterministic.[12] Born emphasizes that this definition of determinability differs from the traditional definition by the change in the order in which the limiting transitions are executed for $\varepsilon \to 0$ and $t \to \infty$. In the usual approach, the region of the initial spread is contracted to a point, and the behavior for $t \to \infty$ is then considered (and, of course, complete predictability is achieved).

[2] For example, the clock synchronization effect described by Huygen was used by unscrupulous clockmakers in the seventeenth century.

[3] This identification of concepts is natural if we recall that turbulence, i.e., the random motion of a continuous medium, admits of a finite-dimensional description.

This procedure is, however, unphysical and must be replaced by the following rule: the behavior of the paths and the region of final spread are first determined for given ε and any t, and the initial spread is then allowed to tend to a point and the behavior of the final spread is investigated for $t \to \infty$. If the final spread of paths for $\varepsilon \to 0$ does not tend to zero, the behavior of the system is "uncalculable in advance." Essentially, it is precisely these ideas that also became the basis for the purely mathematical criterion of *unpredictability* and *stochasticity* of a system, i.e. the positive nature of topologic entropy[23] (see below).

The fact that the instability of all, or almost all, paths may lead to stochasticity seems natural for systems conserving phase volume. Indeed, if an arbitrarily small change in the initial conditions leads to an arbitrarily great divergence of the initial and perturbed paths then for a finite phase space (this can be associated with, for example, finite energy), the incompressible phase fluid must undergo mixing, i.e., the paths have nowhere to go and begin to tangle. Physical aspects of the origin of stochasticity in conservative systems are discussed in greater detail in a book by Zaslavskiĭ[13] and in a review article by Zaslavskiĭ and Chirikov.[14] [4)]

For self-oscillatory systems (for which the phase volume is not conserved), the tangling of paths in space seemed, if not impossible, at least highly exotic. This appeared to emerge from the experience gained with systems having a two-dimensional phase space where, indeed, nothing other than simple attractors, i.e. states of equilibrium and limit cycles, can arise. There was even a hypothesis that only systems of this type which have a finite number of limit cycles and states of equilibrium (mathematicians refer to them as Morse-Smale systems[19,21]), are of real interest even when the phase space has a dimensionality greater than two. Whatever their dimensionality, such systems are, in fact, coarse,[21] i.e. the qualitative topologic structure of their phase space does not change for a small change in the parameters of the system.[2] However, it turns out that Morse-Smale systems with phase space dimensionality ≥ 3 are no longer typical.[20,21] This means that they do not occupy the entire space of the parameters (space of the systems), leaving complexities to the bifurcation values of the parameters, i.e. the boundaries between regions with different simple behavior. Moreover, it has been shown that the space of the parameters already of three-dimensional phase flows contains whole regions occupied by systems with strange attractors and nontrivial dynamics. It has thus been shown that the complex motion of a self-oscillatory system may persist under a change in its parameters, i.e. this is neither exotic nor pathological behavior (although the attractors themselves need not be coarse internally—their complex structure will vary under a weak change in the parameters).

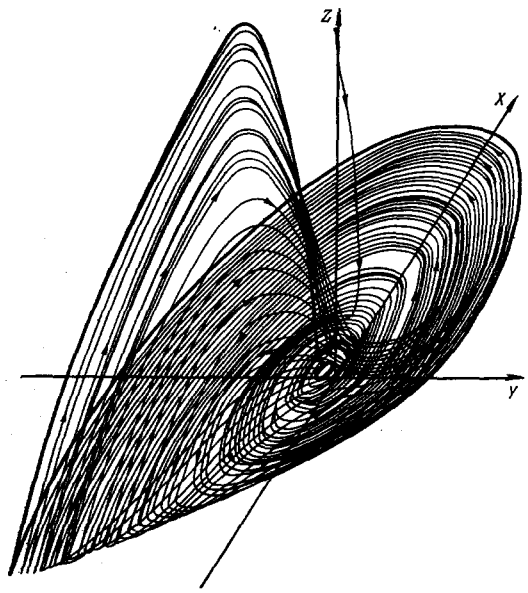

FIG. 1. Example of a "simple" strange attractor [for the system $\dot{x} = z + y + 0.2x$, $\dot{y} = -x + 0.2y$, $\dot{z} = -2z(x+3) + 1$].

In contrast to stochasticity in conservative systems, in the phase space of which regions of stochastic behavior of paths may be in direct contact with regions of dynamic behavior (these are the "islands of dynamics in a sea of stochasticity"[25]), the stochasticity of self-oscillatory systems is *attractive*. This means that, in particular, random behavior may be preceded by a prolonged transient dynamic process. Compression of the phase volume, on the other hand, ensures that the dimensionality of the attractor on which paths terminate for $t \to \infty$ is less than the dimensionality of the phase space.

At least two conditions must be satisfied for a strange attractor to appear in the phase space of a system: (a) all the paths in the neighborhood of a region must enter this region, and (b) almost all the neighboring paths must diverge within this region. On the face of it, these conditions are incompatible. Indeed, they cannot both be satisfied in systems with a two-dimensional phase space: for unstable paths to remain within a bounded region on the phase plane, they would have to "fit" into each other. However, already in three-dimensional phase space such behavior of paths becomes possible: the paths can diverge on a two-dimensional surface, and return by emerging into space. For example, the path can take the form of an untwisting flat spiral whose tail bends into its center and then untwists again (see Fig. 1 and the paper by Rossler[91]). A path of this kind will fill the attractor without closing. We shall show on a simple example that a system will behave stochastically on an attractor of this kind. In doing this, we shall base our discussion on rigorous mathematical results.

a) Stochastic self-oscillator

Consider a self-excited oscillator of the form illustrated in Fig. 2. It is described by the following set

[4)] The mathematical theory of such systems has been developed by Hopf,[15] Anosov,[16,17] Arnold,[7] Sinaĭ,[18] and Moser.[22] We add that conservative systems are those with constant phase volume.

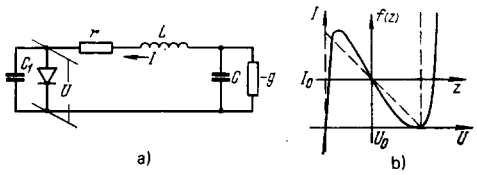

FIG. 2. a) Self-excited oscillator circuit; b) real and idealized (broken line) characteristics of the tunnel diode.

of equations:

$$\left.\begin{aligned} &\dot{x}=y-\delta z,\\ &\dot{y}=-x+2\gamma y+\alpha z+\beta,\\ &\mu\dot{z}=x-f(z),\\ &x=\frac{I}{I_0}-1,\quad y=I_0^{-1}\left[(u_0-u)\sqrt{\frac{c}{L}}+\dot{I}\right],\\ &z=\frac{u}{u_0}-1,\quad \tau=t(LC)^{-1/2}, \end{aligned}\right\} \tag{1.1}$$

where $\delta=(u_0/I_0)\sqrt{c/L}$, $\gamma=(gL-rc)/2\sqrt{LC}$, $\beta=g(u_0/I_0)-1$, $\alpha=1+\beta-2\gamma\delta$, $\mu=\delta c_1/c$, and $f(z)$ is the idealized characteristic of the tunnel diode (Fig. 2b). When the parameter μ in front of the derivative $\dot{z}$ is small, all motions in the phase space of this system divide into slow ones, which correspond to paths on the surface $x=f(z)$, and fast ones, which correspond to the straight lines $x=\text{const}$, $y=\text{const}$. The system has three states of equilibrium for a broad range of values of the parameters α, β, γ, and δ, namely, one at the origin and two located symmetrically on the surface of slow motions. All three are unstable (Fig. 3). If the untwisting of the paths near the unstable foci A and A' is not too rapid, the mapping point cannot leave the region containing all three states of equilibrium: the mapping point moves outward away from the point A along the spiral and, having reached the line $x=\pm1$ along which the surface of slow motion bends over, it enters the neighborhood of the symmetric state of equilibrium A'. It then follows the paths leaving this point and thus returns to the neighborhood of A, and so on. We draw attention to one important point: two paths, lying arbitrarily close to one another near the boundary at which they break off from the slow-motion surface, behave completely differently. Those of them that lie inside the path tangential to the line $|x|=1$ remain on the slow-motion surface and complete one further turn. Other paths that are arbitrarily close to it, but are located outside this tangential path, fall downward (or rise upward) and enter the neighborhood of the symmetric state of equilibrium. It follows that the future of these paths depends on fine details of their past.

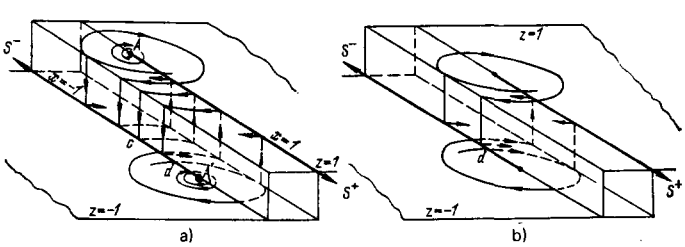

FIG. 3. Phase space of the system given by (1.1) for $\beta=0$, $\mu=0$. a) Two symmetrically situated attractors separated by an unstable limit cycle; b) a single attractor.

For a rigorous demonstration of stochasticity in (1.1), we set $\mu=0$.

By rigorous proof, we mean the following. If, for example, we succeed in showing that the sequence of voltages produced by the self-excited oscillator at discrete instants of time is, in some sense, close to a sequence of independent random quantities, the problem will be solved.

We note that proximity of the solution for the system to a sequence of independent random quantities, say, to a Markov chain, is evidently a manifestation of the strongest stochasticity of the dynamic system. We shall also use a weaker manifestation of stochasticity, namely, the positive nature of topologic entropy, and the property that is useful above all others—the falling off of the autocorrelation function. We add that, if the autocorrelation function falls off exponentially, the system is said to exhibit mixing, and this definitely indicates that the dynamic system is stochastic.[24]

To estimate the behavior of paths in phase space, it is frequently more convenient to consider not the paths themselves but the mapping specified by them of the points of an *intersecting surface* Σ onto itself. In this procedure a correspondence is established between each point and the next point at which the given path again intersects Σ. This is the so-called *sequential mapping* (or Poincaré mapping) and can be written in the form $S_k=F\{S_{k-1}\}$, where S_{k-1} and S_k are the coordinates of successive points on the map. The path is thus observed only at discrete times, i.e., when it intersects the surface Σ. The dimensionality of the space of mapping is less by one than that of the original space which, together with the discrete specification of time, is the advantage of this type of mapping. A limit cycle corresponds to a state of equilibrium under this transformation and a strange attractor should appear as a complicated set of points on the intersecting surface.

We now return to our example. When $\mu=0$, the three-dimensional phase space degenerates into two half-planes overlapping in the band $-1<x<+1$ and the image points pass from one half-plane to the other on the boundaries of the half-planes. The behavior of the paths is then uniquely described by the mapping of the intersecting surface $\Sigma=S^+ + S^-$ onto itself (S^- is the half-line $x=-1$, $z=-1$, $y>-\delta$, and S^+ is the half-line $x=1$, $z=1$, $y<\delta$). Since the motion of each half-plane is described by the equation of a linear oscillator, the required mapping can be easily found in explicit form. It will be discontinuous, i.e., paths that begin and end on Σ can be divided into two groups, namely, (1) those lying on only one of the half-planes, and for them the mapping formula is (we are assuming that $\beta=0$)

$$S_k=T_1S_{k-1}=e^{2\pi\varkappa}S_{k-1}, \tag{1.2}$$

and (2) those passing over into the other half-plane and, for them, the relation

$$S_k=T_2S_{k-1} \tag{1.3}$$

can be defined parametrically:

$$S_{k-1}=\frac{\omega e^{-\varkappa\tau}}{\sin\tau},\quad S_k=2\delta-\frac{\cos\tau+\varkappa\sin\tau}{\sin\tau} \tag{1.4}$$

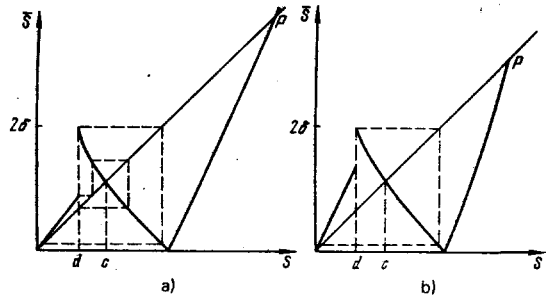

FIG. 4. Sequential mapping for the system given by (1.2).

($\omega = \sqrt{1-\gamma^2}$, $\varkappa = \gamma/a$, and τ is a parameter), so that S_k and S_{k-1} then lie on different half-planes. The resulting discontinuity reflects the pronounced dependence of the paths on their prehistory, which was mentioned above.

However, we shall see that the appearance of the discontinuity on the map is not necessarily required for the existence of stochastic behavior: a different condition is required—the mapping must be a stretching one, i.e., an arbitrarily small strip of Σ must, eventually (after repeated mapping), spread over the entire Σ.[13] This stretching property is clearly connected with the instability of paths in phase space.

It is readily seen that the mapping (1.2)–(1.4) is a stretching one. It is illustrated in Fig. 4 in two qualitatively different cases, namely, $c > T_1 d$(a) and $c < T_1 d$(b), where $d = (T_2)^{-1} 2\delta$ and $c = T_2 c$. In both cases, all paths lying within the region bounded by the unstable stationary point P (it corresponds to an unstable limit cycle in phase space) are drawn into the attractor indicated by the broken line in Fig. 4. In case (a), there are two symmetric attractors separated by an unstable limit cycle (the point c), whereas, in case (b), we have one attractor with the point c in its interior. It follows from (1.2) and (1.4) that $|dS_k/dS_{k-1}| > 1$ and, therefore, there are no stable periodic motions in the attractor. There is, however, a denumerable set of unstable

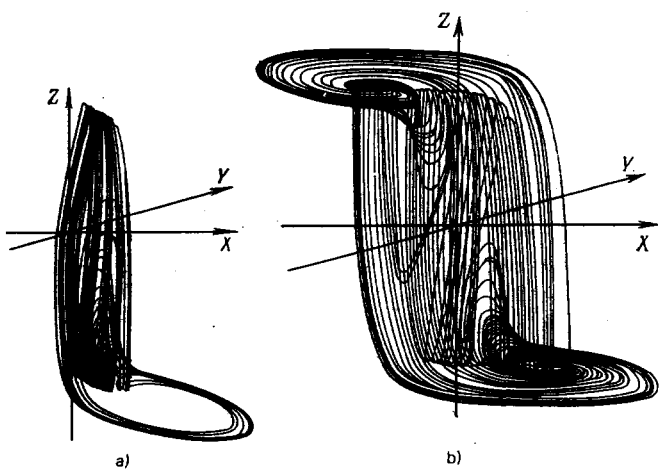

FIG. 5. Phase portraits of attractors obtained by analog simulation of (1.2) with $\mu = 0.1$, $\beta = 0$ [$f(z) = z^3 - z$]. a) $\delta = 0.43$, $\alpha = -0.013$, $\gamma = 0.3$ – two attractors are present (only one of them is shown, for clarity): b) $\delta = 0.66$, $\alpha = -0.33$, $\gamma = 0.35$ – a single attractor.

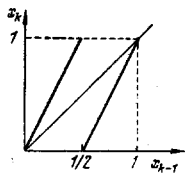

FIG. 6. Nonsmooth mapping of a segment, demonstrating stochastic behavior.

periodic motions between which the mapping point wanders. The mapping corresponding to the interior of the attractor is the stretching mapping of a segment onto itself, which is well known in the theory of dynamic systems. It allows a complete statistical description based on the existence (for all mappings of this type; see Kosyakin and Sandler[28]) of a natural invariant distribution, a probability distribution of a measure, with respect to which the system is ergodic.[5)]

Rigorous results have not as yet been obtained for (1.1) with $\mu \neq 0$. However, computer simulations show that, when μ is small, the system retains stochastic behavior [see Fig. 5, which shows the phase portrait of a strange attractor (1.1) for $\mu = 0.1$, obtained by analog simulation of the system].[6)]

b) Symbolic dynamics

We shall show that the motion of a dynamic system described by a stretching mapping of a segment onto itself can, in fact, be represented by a random sequence. It will be convenient to speak not of this mapping (Fig. 4) but of the analogous symmetric mapping (Fig. 6).

We shall use the methods of symbolic dynamics[22,23] which follow from the work of Hadamard, Birkhoff, and Morse. The basic idea is to code the paths of the system by a sequence of symbols. Let the phase space be divided into a finite number of regions $\Delta_0, \Delta_1, \Delta_2, \ldots, \Delta_{m-1}$ and suppose that a "physical instrument" shows only which of these regions has been reached by the mapping point at a given time. Then, to each point there corresponds a sequence of regions which are traversed by its path at subsequent instants of time. If each such region is placed in correspondence with a "letter" that labels it, then each point will be represented by a "word," i.e., by a sequence of such symbols. If the i-th letter is S, this means that, at time i, the point reaches Δ_s; in this process, i can vary either from $-\infty$ to ∞ or from 0 to $+\infty$.

When the motion is periodic, the sequence of letters in the word is also periodic and, if the motion is stochastic, the sequence will be random.

For the stretching mapping of a single segment onto

[5)] Ergodicity means, in this case, that, in particular, the paths of almost all the points reproduce the entire attractor. However, this cannot be accompanied by mixing (see below).

[6)] The very presence of the strange attractor in the analog simulation suggests that its existence does not depend on a small change in the parameters of the system.

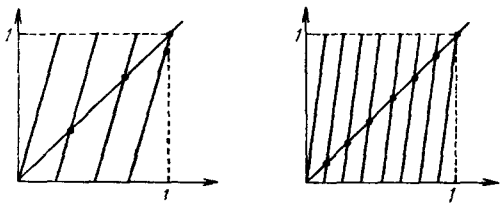

FIG. 7. Results of two- and fourfold application of the transformation of Fig. 6. It is clear that the number of periodic points increases with increasing number of iterations.

itself, one can confine the choice of regions Δ_i, to only two namely $0 \leq x \leq 1/2$ and $1/2 < x < 1$ (Fig. 6). We shall denote them by Δ_0 and Δ_1. We now note that, if the coordinate of a point is written as a binary fraction, then this mapping can be written analytically in the form

$$x_k = \{2x_{k-1}\}, \tag{1.5}$$

where $\{\cdots\}$ represents the fractional part of the number specified as a sequence of zeros and units. For example, this mapping acts on the sequence 0.1001011... as a simple shift (Bernoulli shift) and transforms in into 0.001011.... The fact that the sequence is infinite only to one side and, therefore, the shift is one-sided, is connected with the irreversibility of the transformation (mapping). Its reversible generalization is the two-dimensional baker's transformation resembling the rolling out of dough: a square sheet is rolled out in one direction and is folded; it is then rolled out again, and so on.

If the coordinate x is a rational number, then, beginning with a certain symbol (for example, the n-th symbol), the sequence of zeros and units will repeat, i.e., we have an n-fold periodic mapping point. It is easily verified that the number of periodic points in this mapping is finite and they are everywhere dense and all unstable. This reveals properties that are typical for strange attractors in general: a bounded region from which the paths do not emerge contains a denumerable set of unstable cycles (and not a single stable cycle) which pass the mapping point from one to another.

The easiest way to verify that a stretching mapping of a segment onto itself has a denumerable set of unstable periodic points is to construct successive iterations of this mapping (Fig. 7). Twofold application of the mapping produces four periodic points, threefold mapping produces six, and so on. There are rigorous mathematical theorems relating to this topic[29-31] from which it follows, in particular, that if any continuous (including nonsmooth) stretching mapping of a segment onto itself has a cycle of period three, then it can have a cycle of any period.[7)] It is well known that the sequence of zeros and units defined by (1.5) will be periodic only for a denumerable set of rational numbers, while for almost all irrational numbers, i.e., for most of the points in the segment (0, 1), this sequence will be random in the same sense as the sequence of heads and tails in the classical coin-tossing probability experiment.[58]

Thus, the motions of a dynamic system described by a mapping such as that shown in Figs. 4 and 6 (for example, oscillations in the oscillator of Fig. 2 for $\mu = 0$) can, indeed, be reduced to a random sequence, i.e., they are stochastic.

It is clear that, when symbolic dynamics is developed, the statistical properties of the resulting sequence depend on the choice of the regions Δ_i covering the phase space. In this sense, the statistical description given by it is nonunique. There are, however, stochastic indicators of a dynamic system that do not depend on the choice of Δ_i. One of them is topologic entropy.

c) Entropy of dynamic systems

Let us suppose that a system with continuous time is observed by an instrument (oscillograph) with limited resolution ε (finite spot size on the screen). One cannot then distinguish trajectories $x_1(t)$ and $x_2(t)$ in a time T if the separation between them is less than ε. Let $M(\varepsilon, T)$ be the maximum possible number of different paths, i.e., paths separated by a distance greater than ε. The topologic entropy of the dynamic system, which is described by differential equations, is then given by

$$h_1 = \lim_{\varepsilon \to 0} \lim_{T \to \infty} \frac{\log M(\varepsilon, T)}{T}. \tag{1.6}$$

The subscript 1 means that h_1 is the entropy per unit time; for an arbitrary time, $h_t = |t| h_1$.

From this definition, it immediately follows, in particular, that if a slow path is *stable in the sense of Lyapunov* (i.e., initially close points do not separate to a large distance), the entropy is zero and $M(\varepsilon, T)$ does not in this case increase with increasing T.

If $h > 0$ for the system, then, whatever the precision and length of time for which we "constrain" the path by constant observation, it may, nevertheless, generate a^h different continuations per unit time [a is the base of the logarithm in (1.6)], i.e., it will be unpredictable. Quasiperiodic motion corresponding to an open winding on the torus (with $h = 0$) cannot, therefore, be regarded as stochastic (although it is ergodic).

We emphasize that (1.6) involves the limit as $\varepsilon \to 0$. This means that we retain final unpredictability whatever the precision of observation (provided it is finite). It is only when the precision of observation is infinite ($\varepsilon = 0$) that a system with $h > 0$ will behave in a deterministic fashion.[8)] Since the precision of observation cannot, in principle, be made infinite (if only because this would require infinite energy[34]), it is natural to refer to the behavior of the dynamic systems with $h > 0$ as stochastic.

[7)] Li and Yorke [30] use this in the title of their paper: "Period three implies chaos."

[8)] This is essentially the "physically reasonable" definition of predictability and unpredictability given by Max Born[12] (see above).

Thus, formally, stochastic phase flow differs from predictable flow by the fact that its topologic entropy is greater than zero, and unpredictability jumps discontinuously to a finite value greater than zero as ε increases from $\varepsilon=0$. In the deterministic case, on the other hand, unpredictability increases in a "soft" fashion, increasing from zero together with the observational uncertainty.

We note that, if we take positive topologic entropy as an indicator of stochastic behavior, mixing cannot occur in a stochastic system. The absence of mixing, i.e., complete decoupling of correlations, means only that a dynamic component has been superimposed on stochasticity.

Topologic entropy can also be introduced in the symbolic description of the system:

$$h=\lim_{N\to\infty}\frac{\log K_N}{N}; \tag{1.7}$$

where K_N characterizes the variety of admissible words of length N. In the case of the above Bernoulli scheme, the set of words coincides with the set of all possible infinite sequences of m symbols, $K_N=m^N$, and, consequently, $h=\log m$. Thus the entropy of the stretching mapping of a segment (Fig. 6) is log 2.

The entropy of dynamic systems with invariant measure (K-entropy) introduced by Kolmogorov (as a generalization of the work of Shannon) is intimately connected with topologic entropy. For a broad class of systems, the K-entropy h_μ is equal to the rate of divergence of paths averaged over the given measure μ (more detailed information can be found in Refs. 14, 23, 32, 33).[9)]

d) Butterfly effect

The unpredictability of the behavior of paths chosen by specifying the initial conditions with an arbitrary (but finite!) precision is obviously a fundamental obstacle to long-term nonprobabilistic forecasting. In meteorology, Edward Lorenz referred to this general unpredictability as the "butterfly effect": if the atmosphere is described by a dynamic system with a strange attractor (for example, the Lorenz attractor), even an insignificant change in the initial conditions such as might be produced by the motion of butterfly wings has consequences that would be catastrophic for long-term weather forecasting. This is why computers can produce only a sufficiently short realization of the path of the dynamic system for which the topologic entropy is greater than zero (of course, one can allow the machine to keep on computing as long as necessary but, for large t, the path will no longer be related to the initial segment because entropy cannot be reduced with the aid of a computer!).

Divergence of closely lying paths is a necessary condition for stochasticity. One-dimensional mapping must, therefore, be a stretching one and, if it is required that the paths must remain in a restricted region of phase space, we must introduce first nonsingle-valuedness (so that the return of the path can be arranged) and secondly nonsmoothness.

If, on the other hand, we take a nonsingle-valued but smooth mapping of the segment $0\leqslant x\leqslant 1$, for example,

$$x_{k+1}=ax_k(1-x_k), \tag{1.8}$$

there will, in general, be no stochasticity. The point is that such mapping has a critical point at which $dx_{k+1}/dx_k=0$ and, therefore, stable periodic paths may appear. Nonsingle-valuedness can lead only to a very complicated transient process (connected with the appearance of a denumerable set of unstable cycles when the period three point is created[29-31]; such systems do not contain a strange attractor, but very low-level noise may result in stochasticity because the regions of attraction of stable cycles are small and closely approach one another.[10)]

e) Applications in biology

Many problems in biology, ecology, and genetics[31] lead to the investigation of mappings of a segment. The discretization of time in such problems may be associated with, say, seasonal behavior or successive generations.

For example, in the case of insects, the population x_{t+1} in the $(t+1)$-th generation is related to the population x_t in the preceding generation by $x_{t+1}=F(x_t)$ (in epidemiology, x_t represents the part of the population that has become ill in time t). In economics and in ecology and in biology, there is a tendency toward an increase in x if the preceding population (volume of production in economics) is small, and toward a decrease if it is large. The function $F(x)$ then undergoes a smooth nonsingle-valued mapping of the type described above. It is interesting that natural populations possess mechanisms capable of conserving stable steady-state conditions (this results, for example, from high mortality rates). Laboratory populations, where these factors are modified, can evolve either in accordance with an oscillatory law or randomly.[31]

f) Strange attractors and hyperbolicity

The above discussion and examples may give the impression that discontinuity and nonsingle-valuedness are necessary conditions for a dynamic system to exhibit stochastic behavior. This is not so. We have already mentioned an example that leads to the stochasticity of a single-valued mapping, namely, the

[9)] It is well known that a dynamic system usually has many different invariant measures. The question is—which of them to choose? The answer to this is provided by the variational principle: there exists a measure with maximum K-entropy, and this maximum is just equal to the topologic entropy. In some sense, this situation is analogous to that in ordinary statistical mechanics where maximum entropy is exhibited by the microcanonical distribution. Measures giving maximum K-entropy are therefore referred to as Gibbs measures.[33]

[10)] True stochasticity has been proved for $a=4$ in the case of the above mapping (1.8). The topologic entropy is then equal to log 2.

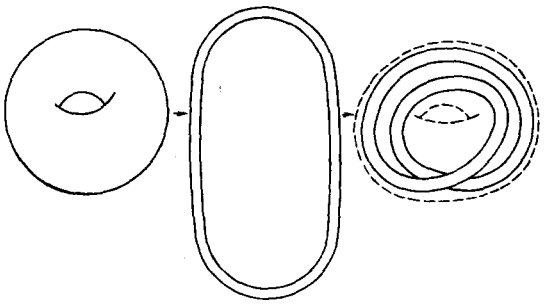

FIG. 8. Smale-Van Danzig transformation. The torus is first stretched to twice its original size and is then inserted into the original torus.

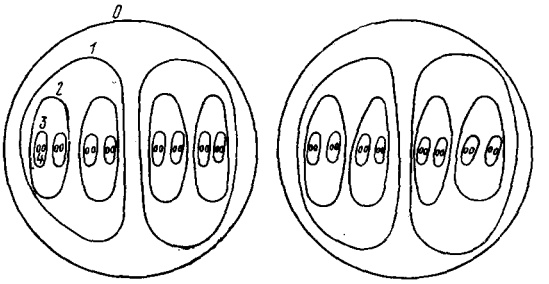

FIG. 9. Cross section of the Smale-Van Danzig attractor after several iterations, giving an idea of the Cantor set.

baker's transformation. Although this transformation is discontinuous, there have been recent examples of smooth plane mappings with strange attractors.[37,98,107] Since these mappings are two-dimensional, there is every reason to suppose that attractive regions with stochastic behavior can appear in smooth dynamic systems (differential equations) already in the case of three-dimensional phase space (the additional dimensionality, as compared with the mapping, is required for motion along the path).

We now consider a graphic example of a strange attractor (in the smooth mapping constructed by Smale and identical with the well-known solenoid of Van Danzig.)[36,19,20,36] This is the mapping of the interior of a torus into itself: the torus is stretched in one direction until its size doubles and is then folded over until it fits into the original torus (Fig. 8). The effect of this mapping along the azimuth is equivalent to the stretching of a segment to double the size (Fig. 6), but two other dimensions are required to ensure that the paths do not intersect when the stretched torus is placed inside the original torus. The result of successive applications of the mapping is illustrated in Fig. 9, which shows the cross section of the interior of the torus. The number of times the mapping of the torus intersects this cross section doubles at each stage and, in the limit, the cross section of the Smale-Van Danzig attractor represents a *Cantor set*.[11)]

The property of hyperbolicity can often be used as a criterion enabling us to determine whether a strange attractor is present in a dynamic system. Hyperbolicity can be roughly defined as a combination of a stretching of the mapped volume in one direction and compression in another. As we have seen, stretching leads to stochasticity, whereas compression is necessary to ensure that the paths remain in a bounded region of phase space. More precisely, hyperbolicity means that two surfaces W^u_x and W^s_x pass through each path $x(t)$. Points on W^s_x approach $x(t)$ exponentially for $t \to \infty$, whereas points on W^u_s approach it exponentially for $t \to -\infty$. These two surfaces are, named respectively, the stable and unstable manifolds of the path $x(t)$. For hyperbolicity, the surfaces must depend on the paths continuously. It is easily seen that hyperbolicity amounts to the transfer to the path of the peropeties of the saddle-point equilibrium state for which W^u and W^s are the separatrices. For the Smale-Van Danzig attractor, W^u is the line along the azimuth and W^s is the surface perpendicular to it.

If the property of hyperbolicity is augmented by a further condition, we obtain Smale's axioma, namely, (1) the set Ω of nonwandering points is hyperbolic,[12)] and (2) periodic points are everywhere dense in Ω. Axiom A could serve as a good indicator of the stochasticity of a system. Systems satisfying this axiom can be investigated quite fully. In particular, continuous dynamic systems obeying axiom A can contain only three types of attractor: (1) equilibrium states, (2) limit cycles, and (3) sets whose topologic entropy is greater than zero (strange attractors). For attractors with axiom A, there are many different invariant measures, and the methods of statistical mechanics[24] can be used to describe them.

To show that an attractor in a system satisfying axiom A is indeed strange, it is, therefore, sufficient to verify that it is not a state of equilibrium nor a limit cycle.

Unfortunately, axiom A is very difficult to verify and, moreover, its requirements are somewhat too stringent. For example, it is not satisfied for the popular Lorenz attractor (see below). There have, therefore, been recent attempts to use softer and more easily verified properties as the criteria of stochasticity.[13,24] However, they are all to some extent analogous to hyperbolicity.

[11)] The "classical" Cantor set is obtained by taking a segment and removing from it the middle third. From each of the remaining "subsegments," one again removes the middle third, and so on. The points remaining after an infinite number of such operations form the Cantor set. It has zero Lebesque measure since the sum of the lengths of the removed pieces is equal to the length of the original interval: $1/3+2/9+4/27+\ldots=1$. The Cantor set is nowhere dense but it cannot be represented by a set of isolated points: it has the capacity of a continuum.

[12)] A nonwandering point is any point such that any of its neighborhoods is traversed by a path originating at this point at least twice and, consequently, an infinite number of times. Nonwandering points correspond to steady states, whereas wandering points correspond to transient processes.

2. PHYSICAL MECHANISMS RESULTING IN STRANGE ATTRACTORS

a) Breakdown of multiperiodic motions-competition, synchronization, and disorder

We now ask: what are the physical mechanisms that impede multiperiodic motions in self-oscillatory systems? The answer to this can be obtained by considering the behavior of an ensemble of weakly coupled quasiharmonic self-excited oscillators:

$$\dot{A}_i = \gamma_i A_i (A_{i0}^2 - A_i^2) + \alpha_i (A_{j,i}, \varphi_{j,i}),$$
$$\dot{\varphi}_i = \omega_i + \beta_i (A_{j,i}, \varphi_{j,i}) \qquad i = 1, 2, \ldots, N; \tag{2.1}$$

where the additions $\alpha(A, \varphi), B(A, \varphi)$ reflect the interaction between the oscillations (modes). When $\alpha = \beta = 0$, all the oscillations are independent and the phase space of (2.1) splits into N phase planes, on each of which there is a unique stable limit cycle with period $2\pi/\omega_i$ and amplitude A_{i0}. In the original $2N$-dimensional space, such independent oscillations correspond to the attraction of the mapping point to an N-dimensional torus, i.e., the product of independent cycles. If all the ω_i are incommensurable, the phase paths on the torus form a dense, nowhere closed, winding, i.e., quasi-periodic motion. This type of attractor is ergodic, but the system does not exhibit stochastic behavior because close paths do not diverge.

On the other hand, if the self-excited oscillators (or self-oscillatory modes) are coupled, this simple quasiperiodic motion will, in general, be disturbed. Depending on the type and strength of coupling, and the proximity of the frequencies of the interacting modes to integeral multiples, can exhibit either a periodic or a stochastic regime can become established in the system as $t \to \infty$ (a limit cycle or a strange attractor will appear in phase space, respectively). However, it is well known that the effects leading to the establishment in the system of interacting self-oscillatory modes of periodic motion, for example, such as competition and mutual synchronization, appear only when the interaction between modes is not too weak. This should also apply to the "mutual stochastization" of modes, i.e., the regime of stable disorder, when the interaction is reduced and eventually removed, should evidently be replaced by the quasiperiodic regime. This means that the Landau-Hopf model of the origin of turbulence will probably be realized for those cases where the amplitudes of the successively appearing pulsations of different scale are restricted by dissipative effects to a level at which interaction with previously appearing pulsations is unimportant.

The simplest single-mode self-oscillations are established in a multimode system as a result of the competition effect connected with the appearance of nonlinear absorption on all or some modes, which progresses as the energy of the "foreign" modes increases. This situation usually arises whenever all the modes draw energy from a single source. The coupling function then can depend only on the mode energy

$$\alpha_i = -A \sum_{j \neq i} \rho_{ij} A_j^2, \tag{2.2}$$

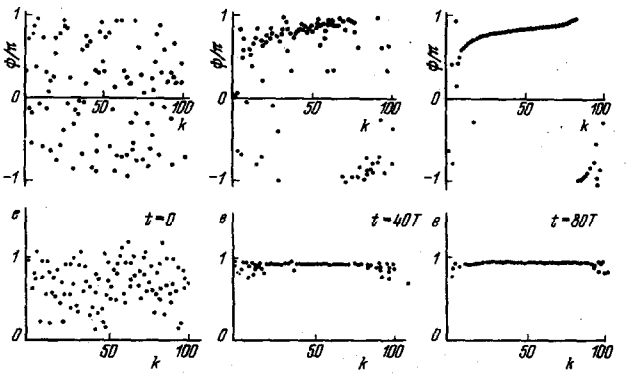

FIG. 10. Synchronization of one hundred coupled self- oscillators with a Lorenz frequency distribution (ψ – total oscillator phase, e – square of amplitude).

where $\rho_{ij} > 0$ is the coupling coefficient. For $\rho_{ij} < \gamma_i$, the coupling is weak and multifrequency generation is possible as, for example, in the gas laser with an inhomogeneously broadened line of the active medium, i.e., different cavity modes are "fed" by different active molecules. If, on the other hand, for example, $\rho_{ij} > \gamma_i$ (strong coupling), the single-mode generation is established independently of the number of initially excited modes. As a rule, the mode with maximum linear growth rate is the most successful. Thus, the striking fact that a simple dynamic regime evolves from the initially generated noise in the nonequilibrium system (medium) is in the first instance, connected with the competition effect.

The synchronization effect also leads to the thinning out and ordering of the oscillation spectrum. In the case of synchronization, the modes do not tend to suppress one another but mutually shift frequencies so that, when nonlinear corrections are taken into account, they either coincide or become commensurable, i.e., limit cycles replace the quasiperiodic winding on the torus. Mutual mode synchronization is possible both in frequency and wave number. In the latter case, the synchronization effect is particularly nontrivial: spatial mode synchronization is, in fact, the explanation of the appearance of complicated ordered structures in non-onedimensional self-oscillatory systems (in particular, the hexagonal prismatic Bénard cells in the case of thermal convection).[13)]

A graphic example of synchronization in an ensemble of a large number of self-excited oscillations is shown in Fig. 10. This figure gives the results of a numerical experiment with the set of equations given by (2.1) in the case of a linear coupling of oscillators with close frequencies when $\gamma_i = A_{i0} = 1$[39]:

$$\alpha_n = \frac{1}{N} \sum_{k=1}^{N} [A_k \cos(\varphi_k - \varphi_n) - A_n],$$
$$\beta_n = \frac{0{,}2}{N} \sum_{k=1}^{N} A_k \sin(\varphi_k - \varphi_n). \tag{2.3}$$

It was assumed that the frequency distribution of the

[13)] Modern physical ideas on convective instability have been reviewed by Normand.[104]

oscillators in the absence of interaction was given by the Lorentz function

$$f(\omega)=\frac{g}{\pi}[g^2+(\omega-\omega_0)^2]^{-1}.$$

It is clear that, if the initial values of the amplitudes A_i and phases $\psi_i=\varphi_i-\omega_0 t$ are random, the single-frequency regime is already practically established as a result of synchronization after 80 periods. Strong enough coupling between the oscillators may result in the opposite effect, namely, randomization. It is just this behavior that is demonstrated by two coupled self-excited oscillators: in the case of very strong coupling, the system can exhibit stochastic self-oscillations (the system then goes over to, for example, the self-excited oscillator with stochastic behavior, which was investigated in Sec. 1).

Let us now consider the most elementary and frequently encountered physical mechanisms that result in the appearance of strange attractors. If we are concerned with the interaction between quasiharmonic self-excited oscillators, then, as a rule, the appearance of "few-mode" stochasticity in dissipative systems requires two factors: namely, resonant coupling between modes and a nonlinear phase drift that inhibits mutual synchronization. However, in contrast to conservative systems,[13,14] disorder in self-oscillatory systems can appear as a result of purely amplitude mechanisms.[43,86] In particular, the appearance of stochasticity as a result of dissipative inertia of individual resonantly coupled modes is quite typical. We shall examine specific examples in the order of increasing "complexity" of the nature of mode coupling. Obviously, the simplest situation is that of linear coupling of modes with close frequencies ω and $\omega+\Delta\omega$. We shall take the example of a laser situated in an external periodic field to show that this coupling plus the inertia of the medium does, indeed, lead to stochastic behavior. We shall then consider mode coupling in the case of multiple frequencies ω and 2ω, and the nondegenerate three-mode interaction of the form

$$\omega_1+\omega_2=\omega_3+\Delta\omega,\quad \mathbf{k}_1(\omega_1)+\mathbf{k}_2(\omega_2)=\mathbf{k}_3(\omega_3). \tag{2.4}$$

In conclusion of this section, we shall briefly discuss the mechanisms of wave turbulence.

b) Forced synchronization and stochastization of pulsations in lasers

Weak linear coupling between Thomson oscillators can lead only to their mutual synchronization.[61] In the approximation in which the field of one of the oscillators is given, this is simply *frequency locking*.[2] Only the two-period regime (beats) can exist outside their locking (synchronization) band. The stochastic behavior of a nonautonomous oscillator may result, for example, from the inertia of its nonlinear characteristic. To verify this, consider the simple model of frequency locking by a resonant external field in a laser.

We shall suppose that the polarization relaxation time T_2 is small in comparison with the field and population-difference relaxation times T_c and T_1, and will use the approximation of a spatially-homogeneous field and

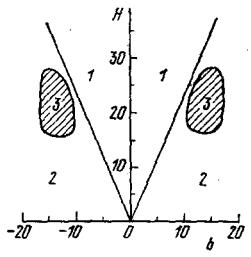

FIG. 11. Plane of external field versus detuning. Figure shows regions of existence and stability of the regimes of stationary generation (1), periodic modulation (2), and random modulation (3) in the system described by (2.6).

single-mode generation. The field amplitude ε at the frequency ω of the external "force" and the population difference N then satisfy the equations

$$\begin{aligned}\dot{\varepsilon}+\left(\frac{1}{2T_c}+i\Delta\omega\right)\varepsilon&=\frac{\omega_{21}d_{21}^2T_2}{2\hbar}N\varepsilon+i\sqrt{\frac{2P_{in}\omega}{Q_{c\,in}}},\\ \dot{N}+\frac{N-N_0}{T_1}&=-\frac{d_{21}^2T_2}{\hbar^2}N\varepsilon\varepsilon^*;\end{aligned} \tag{2.5}$$

where $\Delta\omega$ is the detuning of the external field frequency from the cavity frequency, ω_{21} is the transition frequency, P_{in} is the strength of the external signal at the frequency ω, and Q_{cin} is the Q-factor representing the coupling between the external field and the cavity resonator.[56] If we substitute the dimensionless variables $X+iY=(d_{12}\sqrt{T_1T_2}/\hbar)\varepsilon$, $Z=\omega T_2T_cd_{12}^2N/\hbar$, $\tau=t/T$, $a=T_1/2T_c$, $b=\Delta\omega T_1$, $H=(T_1d\sqrt{T_1T_2}/\hbar)\sqrt{2P_{in}\omega/Qc_{in}}$ into (2.6), we obtain the following set of equations which is similar to (1.2):

$$\left.\begin{aligned}\dot{X}&=a(Z-1)X+bY,\\ \dot{Y}&=a(Z-1)Y-bX+H,\\ \dot{Z}&=Z_0-Z(1+X^2+Y^2).\end{aligned}\right\} \tag{2.6}$$

In the autonomous regime, i.e., when $H=0$, it is easily verified that this system will generate regular damped pulsations[56] when the pumping exceeds the threshold ($Z_0>1$). When $H\neq 0$, the system can support three qualitatively different regimes: stationary generation (stable nontrivial equilibrium states), periodic pulsations, i.e., spikes [limit cycles in the phase space of (2.6)], and random pulsations (strange attractor in the phase space).

The limit of existence of only the simplest of these regimes, namely, stationary generation, can be found analytically on the plane of the parameters. Nonstationary regimes on the other hand, have been investigated in a computer simulation. The resulting subdivision of the plane of the parameters (external field strength, detuning) in the region in which different regimes are observed is shown in Fig. 11.

Figure 12 shows a typical phase portrait of one of the strange attractors. Such attractors evidently exist only in the region of moderate detuning and external fields. In strong fields, the inertia of the population difference has little effect, and forced synchronization sets in as in the usual Thomson oscillator.[83] When the detuning is large, the population difference does not have time to react to changes in the field and one observes the regime of beats (spikes) which is also exhibited by the usual self-excited oscillator outside the

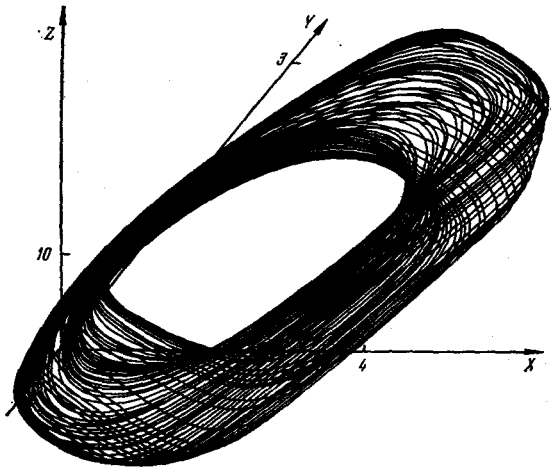

FIG. 12. Phase portrait of the attractor corresponding to the stochastization of a laser by an external field: $a=1000$, $b=40$, $H=85$, $z_0=2$.

locking region. In the same region when the characteristic times for the change in the field and in the population difference are of the same order, one observes stochastic regimes. The parameters for which they exist are quite typical and can be realized:[14] $T_1/T_c \approx 2000$, $P_{in} \lesssim 1W$, smaller excess above threshold.

c) Decay mechanism for the appearance of stochasticity

We now consider second-harmonic generation in nonlinear media. If the medium is in equilibrium, the fundamental wave and the harmonic will periodically exchange energy during the interaction process, or the energy of the fundamental mode will be irreversibly transferred to the harmonic under suitable initial conditions and complete synchronization. In nonequilibrium media, there can be a great variety of interactions between the wave and its harmonics.[15] We shall confine our attention to the case when the nonequilibrium nature of the medium manifests itself only in a finite growth rate for the harmonic whilst the fundamental wave is damped in the linear approximation. The nature of the nonlinear coupling between the waves will be assumed to be the same as in the equilibrium medium. When the synchronization conditions $\mathbf{k}_2=2\mathbf{k}_1$, $\omega_2=2\omega_1-\delta_1(\delta_1/\omega_1\ll 1)$ are satisfied, the complex amplitudes $a_{1,2}(t)$ of the fields $e^{i(\omega_{1,2}t-\mathbf{k}_{1,2}\mathbf{r})}$ will satisfy the equations

$$\left.\begin{aligned}\dot a_1 &= i\sigma_1 a_2 a_1^* e^{i\delta_1 t}+i\alpha_1 a_1(|a_1|^2+\rho_1|a_2|^2)-\nu a_1,\\ \dot a_2 &= i\sigma_2 a_1^2 e^{-i\delta_1 t}+i\alpha_2 a_2(|a_2|^2+\rho_2|a_1|^2)+\gamma_2 a_2,\end{aligned}\right\} \tag{2.7}$$

where all the coefficients are real and $\sigma_1\sigma_2>0$. The terms that are cubic in the amplitude represent nonlinear frequency shifts (nonlinear desynchronization). Let us suppose, for simplicity, that the waves interact only in a resonant fashion and that the self-interaction is appreciable only for the fundamental wave, i.e., $\alpha_2=\rho_1=0$. In real form, we then obtain the following

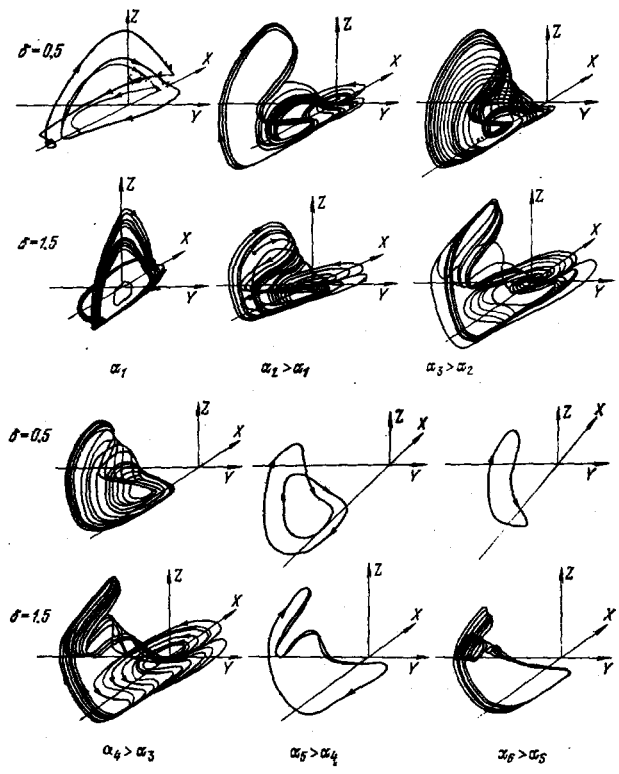

FIG. 13. Different regimes of the system described by (2.8). The paths seem to lie on the surface but, in point of fact, they form a Cantor set in the cross section.

equations instead of (2.7):

$$\left.\begin{aligned}\dot X &= Z-2Y^2+(\delta-\alpha Z)Y+\gamma X,\\ \dot Y &= 2XY-(\delta-\alpha Z)X+\gamma Y,\\ \dot Z &= -2Z(X+1);\end{aligned}\right\} \tag{2.8}$$

where $X=(\sigma_1/\nu)|a_2|\sin\psi$, $Y=(\sigma_1/\nu)|a_2|\cos\psi$, $Z=(\sigma_1\sigma_2/\nu)|a_1|^2$, $\psi=\arg a_2-2\arg a_1-\delta$, $\gamma=\gamma_2/\nu$, and $\delta=\delta_1/\nu$ characterizes the linear and $\alpha=-(2\alpha_1/\sigma_1\sigma_2)\nu$ the nonlinear detuning from synchronism. Stabilization of the unstable harmonic through energy transfer down the spectrum is possible only for $\gamma\leq 0.6$ and α or $\delta>0$.[16] For greater detunings, $\delta\geq 2$ or $\alpha\geq 5$, we have the static stabilization regime. It corresponds to the stable equilibrium states of the system (2.8). When the detuning is smaller, all three equilibrium states of this system are unstable, and the periodic regime or stochasticity appears.[40] Since the mean energy flow in this process occurs down the spectrum, the mechanism responsible for the appearance of stochasticity in this case is naturally referred to as the decay mechanism.

Figure 13 shows typical attractors of the system (2.8), revealed by a numerical experiment with $\gamma=0.25$ and different α, δ. It is clear that a change in α and δ is accompanied by a large number of transitions between periodic and stochastic motions. For example, when $\delta=0.3$ and $\gamma=0.2$, the static stabilization regime sets in for $0\leq\alpha\leq 0.1$ (the equilibrium state is $O_1(-1, Y_1, Z_1)$, where $Y_1\approx 1$ is a stable node). With increasing α, periodic energy transfer between the

[14] They correspond to solid-state lasers.[56]

[15] We recall as an example the simultaneous growth of harmonics leading to their becoming infinite in a finite time. This is the explosive instability.[38,94]

[16] When $\delta=0$, $\alpha=0$, stabilization is impossible even when the harmonic grows very slowly, i.e., γ is arbitrarily small.[41]

FIG. 14. Result of a numerical integration of (2.9) for $\gamma = 0.2$, $\delta = 0.5$, $\alpha = 0.17$. The periodic segments correspond to the motion of the path near unstable cycles.

modes is established, i.e., a cycle (O_1 transforms into a saddle-point focus). The period of the motions is then doubled, and a further increase in α results in the appearance of stochasticity, i.e., a strange attractor, in the dynamic system of two resonantly coupled oscillators. Subsequent increase in α leads to these transitions being repeated in reverse order and the only equilibrium state that becomes stable is $O_2(-1, Y_2, Z_2)$, where $Y_2 < 0$.

The structure of the attractors was investigated with the aid of the Poincaré mapping of the intersecting plane plane $X = -1$. In most cases, random behavior was found to be connected with the appearance inside the attractor of a denumerable set of unstable periodic motions corresponding to saddle-point cycles.[17] Such cycles of different period have also been "observed" in a numerical experiment: for example, the realization of Fig. 14 shows a random sequence of segments of periodic motions. A gradual increase in the precision of the mapping shows that the observed attractors in the section have the structure of a product of a Cantor set and a segment which, as mentioned in section 1, is typical for many strange attractors. It also turns out that both continuous and discontinuous mapping of the $X = -1$ plane onto itself may correspond to stochastic behavior of the system. In the latter case, we have the "separator" mechanism, first discovered by Lanford and Sinaĭ for the Lorenz attractor (see below).

The above process of interaction between a wave and a harmonic is a special case of the nondegenerate three-wave interaction for which the synchronism condition are written in the form given by (2.4). If the high-frequency mode has a growth rate, and the damping of the low-frequency modes is the same, ω_1 and ω_2 will synchronize, and the problem will completely reduce to the analysis of the system (2.8). Stochasticity has been found in this system only for nonzero nonlinear detuning. If, however, the damping of the low-frequency modes is different, then, instead of (2.8), we have already a fourth-order system which can support stochastic behavior even for $\alpha = 0$. The role of nonlinear detuning, which substantially tangles up the motion, is here played by the inertia of the damped modes.

The decay mechanism for the origin of stochasticity is realized essentially independently of the nature of

TABLE I.

Convection 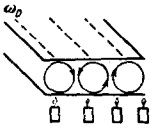	$\mathrm{Ra} = \frac{g\beta\Delta T h^3}{\nu\varkappa}$ $\mathrm{Pr} = \nu/\varkappa$	Equilibrium state	Stationary convective shafts	Oscillatory convection regime	Turbulence
Couette flow 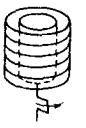	$\mathrm{Te} = \frac{\Omega r l^3}{\nu^3}$	Laminar flow	Taylor vortices	Azimuthal modes	Turbulence
Boundary layer 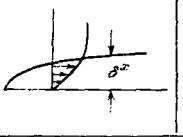	$\mathrm{Re} = \frac{V\delta^*}{\nu}$	Laminar flow	Two-dimensional Tollmien-Schlichting waves	Benney vortices	Turbulence
Wake 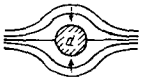	$\mathrm{Re} = \frac{Vd}{\nu}$	Laminar flow	Pair of vortices	Von Karman street	Turbulence

instability of the high-frequency mode.[18] In particular, stochasticity appears even when the instability is parametric.

d) Stochastic stage of parametric instability in plasmas and the Lorenz model

The decay interaction between linearly damped and growing modes leads to stochasticity also in the well-known Lorenz model. We shall now examine the properties of this model and its physical applications.

The system investigated by Lorenz is obtained from the Boussinesq equations describing thermal convection in a horizontal layer heated from below (see the diagrams in Table I) if we confine our analysis to two-dimensional motions, and the flow function ψ and temperature change δT are written in the form[35,46]

$$\psi(x, z, t) = \psi_{11}(t) \sin\frac{\pi x a}{l} \sin\frac{\pi z}{l},$$
$$\delta T(x, z, t) = \theta_{11}(t) \cos\frac{\pi x a}{l} \sin\frac{\pi z}{l} - \theta_{02}(t) \sin\frac{2\pi z}{l}. \qquad (2.9)$$

This representation takes into account three coupled spatial modes, of which two, namely, ψ_{11} and θ_{11}, grow as a result of convective instability for $\mathrm{Ra} > \mathrm{Ra}_I$, while the third, i.e., θ_{02}, is damped. The parameter $a = 1\sqrt{2}$ is the characteristic scale of the modes that are the first to lose stability for $\mathrm{Ra} \geq \mathrm{Ra}_I$ (Ra_I is the first critical Rayleigh number; see Section 3).

Instability is restricted in this case by the transfer of energy (decay) of growing modes to the mode θ_{02}, which corresponds to a change in the main temperature profile (this is the hydrodynamic analog of the well-known quasilinear relaxation effect). The ampli-

[17] Saddle-point cycles appear in the neighborhood of the doubly asymptotic path of saddle-point foci at the origin of coordinates and at the point O_1.

[18] The growth of the unstable mode must, however, be fast enough in comparison with the damping of the subharmonic.

tudes of these modes, $X \sim \psi_{11}$, $Y \sim \theta_{11}$, and $Z \sim \theta_{02}$ satisfy the Lorenz set of equations[35,19]

$$\begin{array}{lccc} \dot{X} = & -\sigma X & +\sigma Y & \\ \dot{Y} = & -Y & +rX & -XZ \\ \dot{Z} = & -bZ & & +XY \\ & \text{I} & \text{II} & \text{III} \end{array}, \qquad (2.10)$$

where σ is the Prandtl number, $r = \mathrm{Ra}/\mathrm{Ra}_r$ is the Rayleigh number normalized to the critical value, and $b = 4/(1+a^2)$ (see Sec. 3). Column I gives the terms responsible for linear mode damping, column II gives those responsible for parametric excitation, and column III those responsible for the nonlinear transfer of energy to the damped mode Z. This system demonstrates stochastic self-oscillations with a strange attractor[20] for a finite range of parameters, and is very similar to the classical equation for the three-wave interaction, but the equations for the wave amplitudes are complex, in contrast to (2.10). However, as we shall see, this difference is not always essential.

We now consider another example, namely, the parametric excitation of waves in magnetoactive plasma.[43] Here, the waves are pumped by a whistler propagating along the magnetic field. Ion sound a_2 and a plasma wave a_1 at the frequency of the lower hybrid resonance are excited in the field of this whistler. These waves, in turn, produce a resonant triple with another plasma wave a_3. In dimensionless form, and in the case of exact synchronism, the equations for the complex amplitudes $a_{1,2,3}$ of these waves can be written in the form[43] (assuming that the fields are spatially homogeneous)

$$\left.\begin{aligned} \dot{a}_1 &= -\nu_1 a_1 + h a_2^* - a_2 a_3, \\ \dot{a}_2 &= -\nu_2 a_2 + h a_1^* + a_1 a_3^*, \\ \dot{a}_3 &= -a_3 \qquad\quad + a_1 a_2^*, \end{aligned}\right\} \qquad (2.11)$$

where h is proportional to the pumping amplitude. This set of equations has a remarkable property: as $t \to \infty$, the linear phase combinations are found to vanish, i.e., the phases lock:[21]

$$\begin{aligned} &\arg a_1 + \arg a_2 \to 0, \\ &\arg a_1 - \arg a_2 - \arg a_3 \to 0. \end{aligned} \qquad (2.12)$$

If we set one of the phases equal to zero, we may regard all the amplitudes $a_{1,2,3}$ as real. Equations (2.11) will then differ from the Lorenz system only by the single additional term YZ in the equation for X ($X \sim a_2$, $Y \sim a_1$, $Z \sim a_3$). Qualitative analysis and numerical simulations have shown, however, that this difference is not fundamental and the solutions of (2.12) and (2.11) behave similarly to the solutions of the Lorenz system. Appearance of stochasticity in this system is then in no way connected with phase drift. The inertia of the parametrically coupled waves plays the leading role here.

The problem of laser dynamics in its simplest formulation is also found to reduce directly to (2.10).[44,45] The interaction between a progressive electromagnetic wave and an inverted two-level system with the wave frequency equal to the transition frequency is described by

$$\left.\begin{aligned} \dot{E} &= \frac{1}{T_c}(P - E), \\ \dot{P} &= \frac{1}{T_2}(EN - P), \\ \dot{N} &= \frac{1}{T_1}\left[\alpha - N - \frac{\alpha - 1}{2}(EP^* + P^* E)\right]; \end{aligned}\right\} \qquad (2.13)$$

where E and P are the dimensionless complex amplitudes of the field and of the polarization of the medium, N is the population difference, α is the ratio of the population difference maintained by the pumping in the absence of the field to the critical value, T_c is the field damping time, and T_1, T_2 are the longitudinal and transverse relaxation times. It can be shown[56] that, as $t \to \infty$, the phase difference between the polarization and the field tends to zero, i.e., E and P can be looked upon as real. The set of equations given by (2.13) then reduces exactly to the Lorenz system (2.10) if we substitute $N \to \alpha - Z$, $E \to [T_1/T_2(\alpha-1)]^{-1/2} X$, $P \to [T_1/T_2(\alpha-1)]^{-1/2} Y$, $t \to T_2 \tau$, where the role of the Rayleigh number is now played by the excess of the population difference above the threshold value $\alpha = r$, and the role of the Prandtl number is played by the ratio of the polarization and field relaxation times $T_2/T_c = \sigma$; $T_2/T_1 = b$ is a characteristic of the medium. We note at once that the parameters for which Lorenz found stochasticity in (2.10) are unrealistic for a laser: $\alpha = 27$ is too high and $T_2/T_c = 10$ presupposes that the linewidth of the medium is narrower by an order of magnitude than the cavity linewidth.[22]

e) The Lorenz attractor

We shall now discuss in greater detail the properties of solutions of (2.10), following mainly the work of Lanford,[47] Afraimovich *et al.*,[48] Vul and Sinaĭ,[49] Guckenheimer *et al.*,[50] Williams,[51] and Guckenheimer.[52]

The set of equations given by (2.10) has a number of properties that substantially simplify the analysis:

I. The system is unstable at infinity and the phase space includes a "sack" which all paths enter: by substituting $u = x^2 + y^2 + (z - r - \sigma)^2$, we find from (2.10) that $\dot{u} \leqslant -C_1 u + C_2 (C_{1,2} > 0)$, i.e., all trajectories enter the sphere $u \leqslant C_2/C_1$.

II. The phase volume of (2.10) contracts uniformly

$$\frac{\partial \dot{x}}{\partial x} + \frac{\partial \dot{y}}{\partial y} + \frac{\partial \dot{z}}{\partial z} = -(1 + \sigma + b), \qquad (2.14)$$

i.e., the attractive set—the attractor—has zero volume.

---

[19] The method used to derive such equations from the Boussinesq equations is discussed in Section 3.

[20] Lorenz found stochastic behavior in (2.10) for $r = 27$, $\sigma = 10$, and $b = 8/3$.

[21] This is easily shown: let $\chi = \mathrm{Im}\,(h a_1 a_2) \sim \sin(\arg a_1 + \arg a_2)$, $\zeta \sim \mathrm{Im}(a_1^* a_2 a_3) \sim \sin(\arg a_2 + \arg a_3 - \arg a_1)$. We then have $(d/dt)(\chi + \zeta) = -(\nu_1 + \nu_2)\chi - (1 + \nu_1 + \nu_2)\zeta$, i.e., all the paths on the χ, ζ plane enter the angle between the straight lines $\chi + \zeta = 0$, $(\nu_1 + \nu_2)\chi + (1 + \nu_1 + \nu_2)\zeta = 0$. However, in this region sign $[(d/dt)(\arg a_1 + \arg a_2)] = -\,\mathrm{sign}\,[\sin(\arg a_1 + \arg a_2)]$; and, consequently, $\chi \to 0$ and $\zeta \to 0$, which leads to (2.12).

[22] However, a similar situation is characteristic for masers.[56]

III. The system is symmetric under space inversion $x \to -x$, $y \to -y$.

We now consider the dependence of the behavior of the system on the parameter r (the Rayleigh number). For $r<1$, the only state of equilibrium is the stable node at the origin $O(0, 0, 0)$. When $r>1$, the origin becomes a saddle-point, and two stable equilibrium states

$$C^{\pm}=(\pm\sqrt{b(r-1)},\quad \pm\sqrt{b(r-1)},\quad r-1),$$

appear at the origin and correspond to stationary convection in the form of shafts with opposite directions of rotation of the liquid.

These nontrivial equilibrium states exist for any $r>1$, but are stable only for $r<r^*=\sigma(\sigma+b+3)/(\sigma-b-1)$ (for $\sigma=b+1$, we have $r^*=\infty$).

When $r=r^*$, unstable cycles (inverse Hopf bifurcation), which existed in the neighborhood of the equilibrium states C^+ and C^-, stick to them and transfer to them their instability. For $r>r^*$, these equilibrium states are saddle-point foci: the one-dimensional separatrix is stable, but the two-dimensional separatrix is an untwisting spiral. Thus, for $r>r^*$, all the equilibrium states in the interior of the above "sack" in the phase space of (2.10) are unstable. The answer to the question as to what attracts the paths in this case requires essentially nonlocal analysis and has been obtained as a result of a numerical analysis of (2.10). It has been found that, for $r>r^*$, all the paths fall on a "ready-made" strange attractor that has already been formed $r<r^*$. The structure of this attractor and the mechanics of its appearance can be understood by reducing the three-dimensional phase flow of (2.10) first to a two-dimensional sequential mapping and then to a one-dimensional nonsingle-valued mapping of the form shown in Fig. 6.[47,49,82] We shall do this for the parameter values chosen by Lorenz, i.e., $r=28$, $\sigma=10$, and $b=8/3$ (for which $r^*=24.74$) when the system exhibits three unstable equilibrium states: O-saddle-point node, which the paths approach along a two-dimensional separatrix surface $W^s(O)$ and leave along the one-dimensional "whiskers" $W^u(O)$, and $C^{\pm}$-saddle-point foci which the paths rapidly approach along one-dimensional separatrices and slowly leave, unwinding along two-dimensional separatrices.

We shall take the $Z=27$ as the intersecting surface Σ

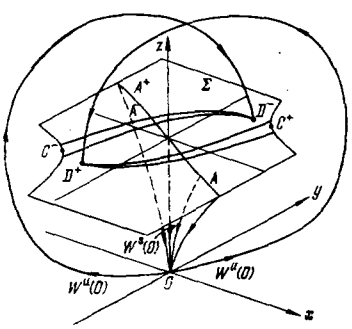

FIG. 15. Phase space of the Lorenz system for $r_2<r<r^*$. $W^s(O)$ and $W^u(O)$ are, respectively, the two-dimensional stable and one-dimensional unstable separatrices of the equilibrium state $O(0, 0, 0)$.

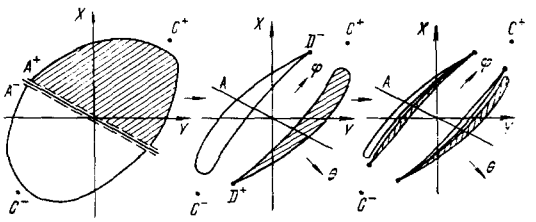

FIG. 16. Mapping constructed by Lanford for the Lorenz system. For clarity, the contraction in the θ direction is greatly reduced: in point of fact, the cross section of the attractor has the appearance of two symmetric "arcs."

passing through the equilibrium states $C^{\pm}$. In the sequential mapping Φ of this plane onto itself, each point departing from the plane Σ downward ($\dot{\Sigma}<0$) is associated with a point at which the given path again intersects Σ in the downward direction. It turns out that the organization of the stochastic behavior of paths is largely determined by the equilibrium state O whose two-dimensional stable separatrix $W^s(O)$ divides the intersecting surface Σ along the line A. Paths issuing from points near A approach very closely the equilibrium state O, but their subsequent fate, whichever of the separatrices $W^u(O)$ they follow out of O, depends on which side of the line A they begin. The mapping is thus discontinuous: points lying on one edge of A (for example, A^+, Fig. 15) are found to merge, and together with the separatrix $W^u(O)$ go to the point D^+, whereas those lying on the other edge go to the symmetric point D^- (the line A is, therefore, referred to as the separator[49]).

It is clear from Fig. 16 that, as a result of the successive iterations of the Poincaré mapping, the initial region is compressed against the attractor in the form of two arcs. Its cross section resembles a Cantor set but, in reality, is a Cantor set for only certain values of the parameters and for a special choice of the cross section. The mapping Φ is thus a combination of stretching in the φ direction (Fig. 16) and compression in the θ direction. We now consider the problem in a less detailed manner by ceasing to distinguish points with the same value of φ and different values of θ, and consider the effect of this mapping only in the φ direction. It is then also convenient to regard as identical the points symmetric with respect to the transformation $x, y \to -x, -y$. The result is a continuous (D^+ and D^- now coincide) but nonmutually single-valued one-dimensional (!) mapping F[23] (Fig. 17). We have already encountered this type of mapping in the last section. The points c, d, and a of the mapping F correspond to C, D and the line A of Φ. When the metric is suitably chosen, F will be uniformly stretching; this means that the attractor indicated by the broken line is a strange attractor. The mapping Φ was recently shown[109] to be a mixing one,

[23] The transition from Φ to F is analogous in this case to the transition from the Smale-Van Danzig mapping (Fig. 9) to the stretching of a segment (Fig. 6). Mathematically, this transition is rigorously described by constructing the inverse limit.[36,51,52]

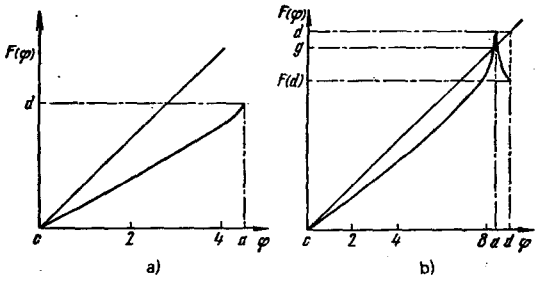

FIG. 17. One-dimensional nonsingle-valued mapping obtained for (2.10) (no strange attractor): *a*) $r=10$, *b*) $r=15$.

and F has a positive topologic entropy. The one-dimensional mapping F provides a clear illustration of all the main properties of the Lorenz attractor. For example, it follows from it that this attractor is noncoarse: indeed, the point a need not be periodic [since the separatrix $W^u(O)$ is then everywhere dense in the attractor], and can become periodic for an arbitrarily small perturbation of the parameters (when $W^u(O)$ returns to zero).

We now examine the appearance of an attractor as r increases with $b=8/3$ and $\sigma=10$ (this was first done by Afraimovich *et al.*[48] and independently by Kaplan and York[101]).

For $1<r<r_1\approx 13.926$, when $F(a)=d<a$, the mapping has the form of Fig. 17a and all the paths are attracted to the point C (i.e., to the states of equilibrium $C^\pm$). When $r=r_1$, we have bifurcation, i.e., $F(a)$ becomes equal to a and this corresponds to the return of the separatrix $W^u(O)$ to the saddle-point (0, 0, 0). This is accompanied by the appearance of an unstable cycle (point g in Fig. 17b).

For $r_1<r<r_2\approx 24.06$, the mapping F has the form shown in Fig. 17b. This mapping no longer contains stochasticity: it is a stretching one for $g<\varphi<b$, and there is an ergodic point of period 3. The appearance of stochasticity is now connected with the appearance of a homoclinic contour, i.e., paths running from one of the unstable cycles to another (on the mapping F, this corresponds to points that are doubly asymptotic to g).[48,53] However, the stochasticity in this range of the parameter r is not as yet attractive because $F(d)<g$, and practically all the points from the region $g<\varphi<d$ depart to the stable equilibrium state C.

The next bifurcation ($r=r_2$) occurs when $F(d)=g$ and the separatrix $W^u(O)$ winds itself on an unstable cycle. The homoclinic contour vanishes, but the stochasticity

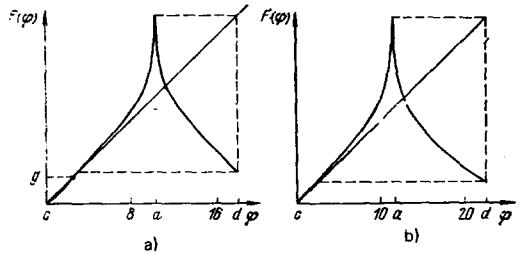

FIG. 18. One-dimensional mapping for (2.10) when a strange attractor is present: *a*) $r=24.3$, *b*) $r=28$.

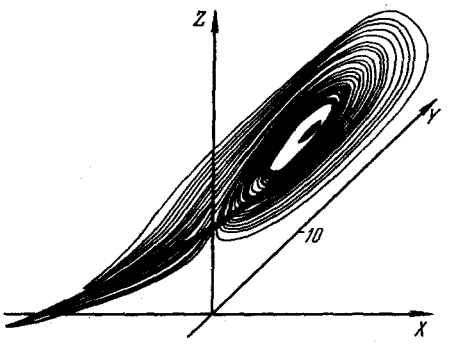

FIG. 19. Portrait of a strange attractor of (2.12), showing regions of attraction of the equilibrium states C^+ and C^-.

generated by it remains and becomes attractive, i.e., a strange attractor appears. Thus, the Lorenz system contains three attractors for $r_2<r<r^*$, namely, two simple ones and a strange one (shown by the broken line in Fig. 18a). This means that, depending on the initial conditions, either a stochastic or a dynamic regime is realized. Transition to stochasticity is accompanied by hysteresis which is characteristic of the hard regime.[24)] When $r=r^*$, the unstable cycle "sticks" to the equilibrium state ($g=c$), and only the strange attractor remains after this bifurcation. Finally, a stable limit cycle appears for $r=r_3=220$. The succession of regimes is illustrated in Fig. 20.

The asymptotic behavior of the Lorenz system for $r\to\infty$ can also be investigated analytically by using the following substitution proposed by V. I. Yudovich:

$$x=\frac{\varepsilon}{\sqrt{2\sigma}}X,\quad q=\frac{\varepsilon^2}{\sigma}\left(\sigma Z-\frac{1}{2}X^2\right),\quad t=\frac{\varepsilon}{\sqrt{\sigma}}t_{\text{old}}. \tag{2.15}$$

The set of equations given by (2.11) then reduces to the equation for a "controlled" pendulum whose frequency depends on its energy in an inertial fashion:

$$\begin{aligned}&\ddot{x}+\varepsilon h\dot{x}+x^3+(q-1)x=0,\\ &\dot{q}=-\varepsilon a q+\varepsilon\beta x^2,\end{aligned} \tag{2.16}$$

where $h=(\sigma+1)/\sqrt{\sigma}$, $a=b/\sqrt{\sigma}$, $\beta=(2\sigma-b)/\sqrt{\sigma}$. Large values of the Rayleigh number in the Lorenz system correspond to small values of ε. The system (2.16) is then quite close to a conservative system with the potential

$$U(x)=\frac{x^4}{4}+\frac{(q-1)x^2}{2},\qquad q=\text{const}.$$

This proximity enables us to investigate the solutions of (2.16) by the averaging method. Analysis of the averaged equations[100] shows that, for each $\sigma>(2b+1)/3$ and sufficiently large r, the Lorenz system supports a stable cycle covering both nontrivial equilibrium states. When $b+1<\sigma<(2b+1)/3$, the neighborhoods of these states each contains a further unstable cycle. Analytically, it follows from these equations that, for $r\to\infty$ and $\sigma=(2b+1)/3$, the system supports a homoclinic figure of eight (two separatrices leaving the point (0, 0, 0) and returning to this point), the decay of

[24)] The form of the phase space with three attractors in the case of (2.12) is shown in Fig. 19.

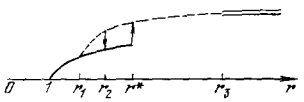

FIG. 20. Evolution of an attractor in the Lorenz system with increasing r for $\sigma = 10$, $b = 8/3$ (solid curve-stable equilibrium state, broken curve-strange attractor, double curve-stable limit cycle).

which leads to the appearance of a denumerable set of cycles and to stochasticity.[25)]

f) Conservative mechanisms

All the physical mechanisms leading to stochasticity which have been discussed so far are fundamentally connected with dissipation of the energy of one of the modes and the supply of energy from external sources to other modes. These are the most important nonconservative mechanisms responsible for the appearance of disorder in, for example, hydrodynamics. At the same time purely conservative mechanisms may also be responsible for the appearance of stochasticity in self-oscillatory systems (in particular, in the case of nonlinear overlapping of resonances[13,14]). The contribution of dissipation and of external sources of energy in this case reduces merely to the choice of one or several of the already existing stochastic motions that are distinguished by the fact that for them energy dissipation and energy consumption are, on the average, equal. The stochastic regime segregated in this way can then be attractive, and a strange attractor may appear in the phase space of the system.[26)] The appearance of a strange attractor in such a situation should resemble the appearance of a limit cycle in a self-oscillatory system close to a nonlinear oscillator, i.e., low nonlinear friction transforms one or more of the existing closed paths into a limit cycle.

It is clear that the spectral characteristics of motion on the attractor produced in this way (independently of whether the motion is periodic or stochastic) can remain the same as for the original conservation motion. In general, it is impossible to distinguish stochastic self-oscillations from the stochastic motion of a conservative system in a steady state.[27)] This can only be done by investigating the process of establishing the stochastic motions in which we are interested.

g) Large number of modes, developed turbulence

The "few-mode" strange attractors which we have investigated so far and whose existence is striking in itself, enable us to examine the mechanics of the development of disorder in dissipative media. However, they are relevant for real turbulence (those forms of it represented by strange attractors) only in the neighborhood of the limit of their appearance. The point is that the number of excited modes on which the turbulence is based increases with increasing degree of non-equilibrium of the medium, i.e., the strange attractor becomes a "multimode" attractor. The question is whether physical mechanisms are capable of supporting the existence of such attractors. Generally speaking, the answer is that they are capable because the number of interacting modes is not very fundamental for the appearance of effects such as competition or synchronization of modes, nonlinear phase drift, and so on, which impede or facilitate the emergence of stable disorder in nonuniform dissipative media. We shall consider two examples taken from the field of wave turbulence.

Flyn and Manheimer[97] have investigated numerically the stabilization of a stable ion-acoustic mode in plasma due to the upward transfer of energy along the spectrum. They considered a model consisting of 10 harmonics (the higher harmonics were nonresonant because of dispersion). The first mode ω had a growth rate γ and the tenth was subject to damping with $\nu = 10\gamma$, i.e., there was an inertial interval[93] of width 9ω. It turned out that both in the presence of dispersion within this interval and in its absence, there was no cascade transfer of energy along the spectrum characteristic of Kolmogorov turbulence, and stationary energy distributions were not established. The resulting picture was exactly the same as for the interaction of a growing and a damped harmonic, mentioned above [see also (3.9)], i.e., the energy of all the modes pulsated randomly, varying by more than two orders of magnitude (see Fig. 30a). However, the phases of all the individual modes turn out to be coupled.[28)]

Numerical simulations have shown that the nature of stochasticity in such models is not very dependent on the number of interacting modes and there is only a change in the width of the region occupied by the stochasticity in the space of the parameters.

The role of phase effects in generating multimode disorder in a dissipative medium can be seen from the following example.[96] Consider the interaction between a low-frequency (Ω_0, q_0) wave and a high-frequency wave with the dispersion law $\omega^2 = v^2k^2 + \omega_0^2$ in a one-dimensional active medium (transmission lines with nonlinear leakage current $j(u) = -\gamma_1 u - \gamma_2 u^2 + \gamma_3 u^3$). Here, $\gamma_{1,2}$ are responsible for the growth of the oscillations in the nonequilibrium medium and γ_3 for the linear damping: Ω_0 and q_0 are fixed (determined by the length of the resonator). The interaction between the low- and high-frequency waves occurs through the resonant coupling between them due to the quadratic nonlinearity ($\gamma_2 \neq 0$) of the leadage current (synchronisms

[25)] The mechanism responsible for the appearance of stochasticity connected with the breakdown of the homoclinic figure of eight has been discussed by Neĭmark[59] in connection with a nonautonomous second-order system.

[26)] The stochasticity of a self-oscillatory system originating from the nonlinear overlapping of resonances was detected experimentally by Papko *et al.*[60]

[27)] In the most general case, this was already predicted by Birkhoff (see Andronov[2]).

[28)] We note that the weak-turbulence approximation, which is based on the hypothesis of random phases of the individual waves, is a method of describing wave turbulence. The question of what are the mechanisms that maintain stochasticity in such a description is usually left open.

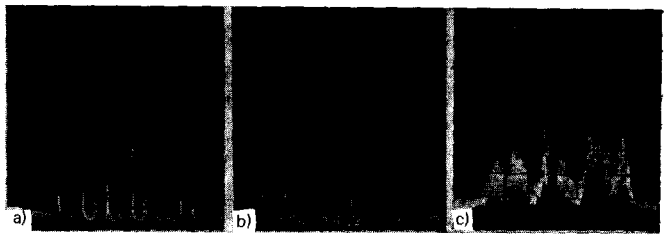

FIG. 21. Abrupt transition from discrete spectrum to continuous spectrum during breakdown of the mode-locking regime.[96]

of the form $\omega_i \pm \Omega_0 = \omega_{j,l} + \Delta_{j,l}\omega, k_i \pm q_0 = k(\omega_{j,l})$). Figure 21 shows the experimental[96] spectra of high-frequency oscillations in this "medium" for different ratios of the quadratic and cubic nonlinearities.[29] When the quadratic nonlinearity is small, mode competition is the predominant effect, and the few-mode dynamic regime is established (Fig. 21a). As γ_2 increases, the high-frequency spectrum becomes increasingly dense (Fig. 21b), and the number N of modes during the initial stage, which are due to explosive instabilities,[94] increases as $\dot{N} \sim N^2$. However, in the present context, the fundamental point is different, namely, it is clear from Fig. 21 that the high-frequency spectrum consists of equidistant lines, despite the presence of strong dispersion in this frequency band. This is due to the mode locking effect which we have already discussed. However, a further increase in the quadratic nonlinearity leads to the appearance of new modes with incommensurable frequencies. This is accompanied by rapid suppression of the mutual mode locking and the development of random self-oscillations characterized by a continuous spectrum (Fig. 21c). Under these conditions, stochasticity develops in the hard manner (and this, in particular, shows its attractive character), i.e., as the ratio $R = \gamma_2/\gamma_3$ increases, disorder sets in for a value of R_2 greater than R_1 (at which it vanishes when this ratio decreases). In the hysteresis region, $R_1 < R < R_2$, we have either an equidistant spectrum or turbulence, depending on the initial conditions (Fig. 21b and c).

3. FINITE DIMENSIONAL DESCRIPTION OF HYDRODYNAMIC TURBULENCE

Hydrodynamic turbulence, described by the Navier-Stokes equations, has very little in common at first sight with the motion of dynamic systems, i.e., with ordinary differential equations with which we were largely concerned above. This connection does, however, exist and is very intimate. Hopf originally put forward the hypothesis that the entire set of paths of the Navier-Stokes equation (its phase space is infinite-dimensional) is attracted to a finite-dimensional set. Hence, it immediately follows that, as $t \to \infty$, the motion of the fluid can be described by finite-dimensional equations. Although it is true that this hypothesis has not so far been verified, it seems perfectly natural if we recall that viscosity impedes the existence of small-scale perturbations. We add that the main bifurcations that have already been established for the Navier-Stokes equation have a finite-dimensional character.[108] This is confirmed, for example, by the transition of stable stationary flow into periodic flow (creation of a limit cycle from an equilibrium state), by establishment of doubly periodic flow (creation of a two-dimensional torus), and so on. There is therefore every reason to suppose that the next bifurcation, i.e., the transition to disordered flow, is also finite-dimensional for many hydrodynamic problems. This is apparently valid for both two-dimensional and three-dimensional flows. However, rigorous results have so far been obtained only for two-dimensional hydrodynamics when the motion is independent of one of the coordinates.

a) Two-dimensional hydrodynamics

According to the results reported by Ladyzhenskaya,[63] all limit regimes (for $t \to \infty$) corresponding to two-dimensional Navier-Stokes equations

$$\mathbf{v}_t - \nu\Delta\mathbf{v} + \sum_{k=1}^{2} v_k \mathbf{v}_{x_k} = -\frac{1}{\rho}\nabla p + \mathbf{f}(x), \quad \operatorname{div}\mathbf{v} = 0, \quad \mathbf{v}|_S = 0 \qquad (3.1)$$

(where S is the bounding contour) are described by a dynamic system that is equivalent to a finite-dimensional system. More precisely, this result can be formulated as follows. If we write $\mathbf{v}(x,t) = \sum_{k=1}^{\infty} a_k(t)\varphi_k(x)$, the motions described by (3.1) can be reconstituted from their projection (*Galerkin approximation*), i.e., $\mathbf{v}_N(x,t) = \sum_{k=1}^{N} a_k(t)\varphi_k(x)$ in N-dimensional Euclidean space, where the $a_k(t)$ satisfy

$$\dot{a}_k = \sum_{l,m} \sigma_k^{lm} a_l a_m + \sum_i \gamma_k^i a_i + f_k. \qquad (3.2)$$

The important feature is that the nature of the original solution $\mathbf{v}(x,t)$ is strictly the same as the behavior of $\mathbf{v}_N(x,t)$: if $\mathbf{v}_N(x,t)$ does not depend on t, then $\mathbf{v}(x,t)$ will not do so either; if $\mathbf{v}_N$ is periodic in t, then so is $\mathbf{v}$; if $\mathbf{v}_N$ is periodic in t, then so is $\mathbf{v}$; if $\mathbf{v}_N(x,t)$ has a continuous spectrum, then $\mathbf{v}(x,t)$ will also have such a spectrum. Thus, the development of two-dimensional turbulence can be rigorously established by investigating the finite-dimensional projection, i.e., (3.2). Naturally, N increases with increasing R. This result is not too difficult to understand physically and is connected with the role of viscosity, which increases with decreasing scale and ensures that small-scale perturbations follow the strong large-scale perturbations.

b) Relation to experiment

Experimentally, the turbulence represented by a strange attractor should be distinguished by the nature of its appearance, i.e., a small number of transitions preceding it and a sharp, "catastrophic,"[30] appearance of random pulsations with a continuous spectrum. Let us consider from this point of view the results of ex-

[29] This ratio can easily be varied by varying the constant bias across the tunnel diodes used as the nonlinear leakage elements.

[30] There exists at present a very interesting topologic theory the "catastrophe theory," developed by Tom[64] and others, which can be used to describe many discontinuous transitions in very different systems.

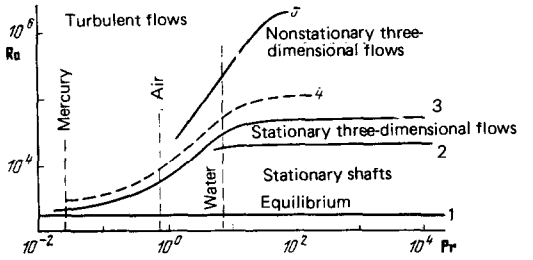

FIG. 22. Regions of existence of different convective regimes in a horizontal layer of liquid heated from below.

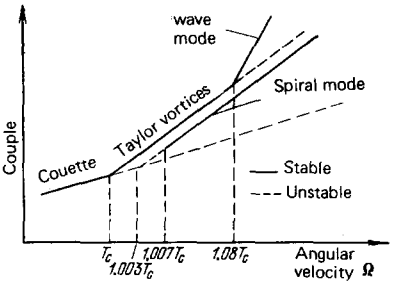

FIG. 23. Couple applied to inner cylinder as a function of the Taylor number. Breaks correspond to changes in flow structure.

periments on the onset of turbulence in classical hydrodynamic flows. We shall see later that the appearance of turbulence during thermal convection, during Couette flow between cylinders, in a boundary layer, and in the wake of a body in a flow does, indeed, frequently resemble the picture prescribed by the "attractor model," i.e., as supercriticality increases, simpler motions are replaced by more complicated motions, and turbulence discontinuously sets in after a small number of transitions.

The analogy between the above transitions will be clear from the table,[65] but they are interesting enough for us to consider them briefly.[31)]

c) Thermal convection

Convective motion in a horizontal layer of liquid or gas heated from below has been under investigation for more than seventy years[66] (Bénard, 1900; Rayleigh, 1916) and can be described by two dimensionless parameters, namely, the Rayleigh number $\mathrm{Ra}=g\Delta Th^3\beta/\nu\varkappa$ and the Prandtl number $\mathrm{Pr}=\nu/\varkappa$, where g is the gravitational acceleration, $\Delta T>0$ is the temperature difference between the lower and upper boundaries of the layer, h is its thickness, ν the viscosity, $\varkappa$ is the temperature diffusivity of the medium, and β the thermal expansion coefficient. Figure 22 shows the subdivision of the plane of the parameters Ra, Pr into regions in which different types of convective motion take place. This subdivision was introduced by Krishnamurti[67] as a result of an analysis of experiments with different liquids and gases, covering values of Pr between 10^{-2} (mercury) and 10^4 (silicone oil). The first transition from hydrodynamic equilibrium to stationary two-dimensional convection does not depend on Pr and, for $\mathrm{Ra}>\mathrm{Ra_I}$,[32)] leads to the appearance of stable structures in the form of convective shafts, i.e., two-dimensional vortices. A further increase in Ra results in the second transition: for $\mathrm{Ra}>\mathrm{Ra_{II}}$, the two-dimensional motions are replaced by three-dimensional stationary regimes corresponding to the excitation of many degrees of freedom, i.e., multimode structures appear; for $\mathrm{Pr}\lesssim 7$, $\mathrm{Ra_{II}}\approx 12\mathrm{Ra_I}$. This stationary regime then goes over into an oscillatory regime for $\mathrm{Ra}\gtrsim\mathrm{Ra_{III}}$. For small values of $\mathrm{Pr}<5$, the stationary multimode convection does not take place,[67] and the stationary single-mode regime is immediately replaced by a nonstationary regime. The structure of the oscillatory regimes in the region between 3 and 5 becomes more complicated (again in a discrete manner) as the degree of nonequilibrium of the system, i.e., Ra, increases. Disordered oscillations with a continuous spectrum of pulsations, i.e., turbulence, set in for $\mathrm{Ra}>\mathrm{Ra_V}$. A further increase in Ra is accompanied by a change in the turbulence structure: apparently new degrees of freedom of the system begin to participate in the motion. For example, experiments with water in the interior of a turbulent region[68] have shown the presence of eight transitions for $1.05\times10^5>\mathrm{Ra}>2.76\times10^5$. Similar transitions have been observed in experiments with low-temperature helium.[69,70] They correspond to breaks in the dependence of the heat flow through the layer (Nusselt number Nu) on the Rayleigh number.

d) Coutte flow between rotating cylinders

This flow is very similar to convection in a layer, and the resulting picture of successive complication of flow and the sudden onset of turbulence is similar to that described above. When only the inner cylinder rotates, the various limits are as shown in Fig. 23, which shows the couple applied to the inner cylinder as a function of the Taylor number $T=\Omega r l^3/\nu^2$, which describes the nature of the flow (Ω, r are, respectively, the angular velocity and radius of the inner cylinder, and l is the gap between the cylinders. The first of the transitions shown in Fig. 23 was observed by Taylor himself[72] nearly half a century ago: for $T\gtrsim T_{\mathrm{I}}$, the "smooth" flow becomes unstable, and structures in the form of rings around the inner cylinder are found to appear. These are the Taylor vortices. The number of these vortices, i.e., the mode number in z, may be different. For $T\gtrsim T_{\mathrm{II}}\approx 1.08T_I$, the vortices become unstable with respect to bending oscillations running along the angular coordinate θ, and azimuthal waves with spatial structure $f(z,\theta)\sim e^{i(mz-n\theta)}$ are found to appear. Depending on the initial conditions, a state with large m and n can appear (Coles[73] observed up to 70 states as

[31)] A detailed discussion of the transitions to turbulence in different hydrodynamic flows is given by A. S. Monin in this issue (p. 429). The author is indebted to A. S. Monin for enabling him to see this paper prior to publication.

[32)] For a layer with isothermal solid boundaries, $\mathrm{Ra_I}=1700$, whereas, for a layer with free boundaries, $\mathrm{Ra_I}=(27/4)\pi^4/4\approx 657$.

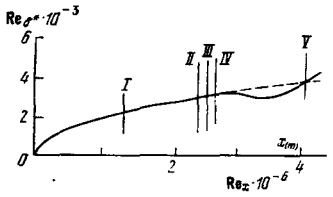

FIG. 24. Transitions to turbulence in the boundary layer.

the angular velocity was varied depending on the prehistory). Turbulence sets in for $T > T_{III}$.[33)]

e) Boundary layer

A finite number of transitions precedes the appearance of turbulence in the boundary layer as well. However, here, the picture is much more complicated.[71,74,75 34)] The transition points are shown in Fig. 24, which plots $\mathrm{Re}_\delta = V\delta^*/\nu$ as a function of the Reynolds number $\mathrm{Re} = Vx/y$, where δ^* is the characteristic thickness of the boundary layer. The Reynolds number increases along the flow. An instability leading to the growth of two-dimensional Tollmien-Schlichting waves[75] appears at *I*. Nonlinear effects have a strong effect at *II* and, as a result of the interaction between two-dimensional and three-dimensional Tollmein-Schlichting waves, the flow becomes vortex-dominated and the so-called Benney vortices are formed.[76] This is accompanied by a point of inflection on the velocity profile. Lower down along the flow (point *III*), the development of secondary instability results in the appearance of small-scale perturbations and small turbulent regions, i.e., turbulent spots, which grow as they move with the flow, appear at *IV*. At Re* (point *V*), a flow with developed turbulence is formed. The structure of the turbulent layer is quite complicated, consists of many layers (it contains a sublayer, a superlayer, and so on[71,74]), and is not as yet completely understood.

f) Wake of a body in a flow

A sketch of the turbulent wake of a body in a flowing liquid was already given by Leonardo da Vinci,[77] but systematic studies of this type of flow began roughly 60 years ago with the work of von Karman.[78,79] Viscous flow of this kind occurs up to $\mathrm{Re} = 4$. For $\mathrm{Re} > 4$, the boundary layer breaks off on either side of the body and forms two symmetric vortices (Fig. 25) which attach themselves to the surface of the cylinder. For $\mathrm{Re} > 40$, the wave perturbation between the "upper" and "lower" flows in the separated boundary layer begins to increase (the cylinder serves only to produce the free boundary layer). The evolution of this perturbation with increasing x resembles the evolution of a simple wave in a nonlinear medium without dispersion: at first, the wave profile becomes increasingly steep and then the wave "turns over," forming a "Karman street" ($\mathrm{Re} \gtrsim 80$). A further change in structure occurs only for $\mathrm{Re} \sim 10^5$ when turbulent regions appear in the wake. For $\mathrm{Re} \approx 5.5 \times 10^5$, the wake of the body becomes completely turbulent.[79]

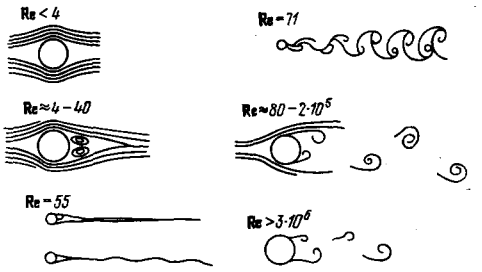

FIG. 25. Transition to turbulence in the wake of a cylinder.

Thus, if we ignore some of the details, turbulence does indeed appear in many of the above flows not in a spectrally evolving manner (as in the Landau-Hopf model), but catastrophically, and is preceded by a small number of qualitatively different regimes. It is still difficult to say what is the relevance of the strange attractor to the appearance of turbulence in, for example, the boundary layer. However, for Couette flow, and in thermal convection, this representation of turbulence is completely realistic. We shall now consider finite-dimensional mathematical models in which the appearance of random pulsations can be observed for such flows.

The simplest and most general method of constructing a finite-dimensional approximation to the equations of hydrodynamics is the Galerkin method.[80,110] Its essence is that the velocity, pressure, and temperature fields are expanded in terms of a finite set of orthogonal functions (most frequently, the eigenfunctions of the linear problem) in which the expansion coefficients a_i are time-dependent. By demanding minimum approximation error, one obtains a set of ordinary differential equations of the form given by (3.2).

The simplest application of this approach is that to convection, where, in the linear approximation, the liquid is at rest and the problem is self-adjoint. The situation is somewhat more complicated in the case of Couette flow between cylinders. For the boundary layer and for the wake of a rigid body in a flow, the linear boundary problem leads to the Orr-Sommerfeld equation, and the determination of the eigenfunctions is not in itself trivial.

g) Turbulent convection in the Hele-Shaw Cell

The Hele-Shaw cell is a parallelepiped, one of the horizontal dimensions of which (d in Fig. 26a) is much smaller than the other two. It is very convenient for graphic experiments. At the same time, convective motions in a cell or gap of this kind are two-dimensional and admit of a detailed theoretical description and subsequent comparison with experiment.[81] At present, convection in the Hele-Shaw cell is among one of the few experiments capable of testing finite-dimensional models of the origin of hydrodynamic turbulence not only qualitatively but also quantitatively (!).

[33)] When the external rather than the internal cylinder is made to rotate, the transition to turbulence is found to be different.[73]

[34)] See also the review by A. S. Monin in this issue (p. 429).

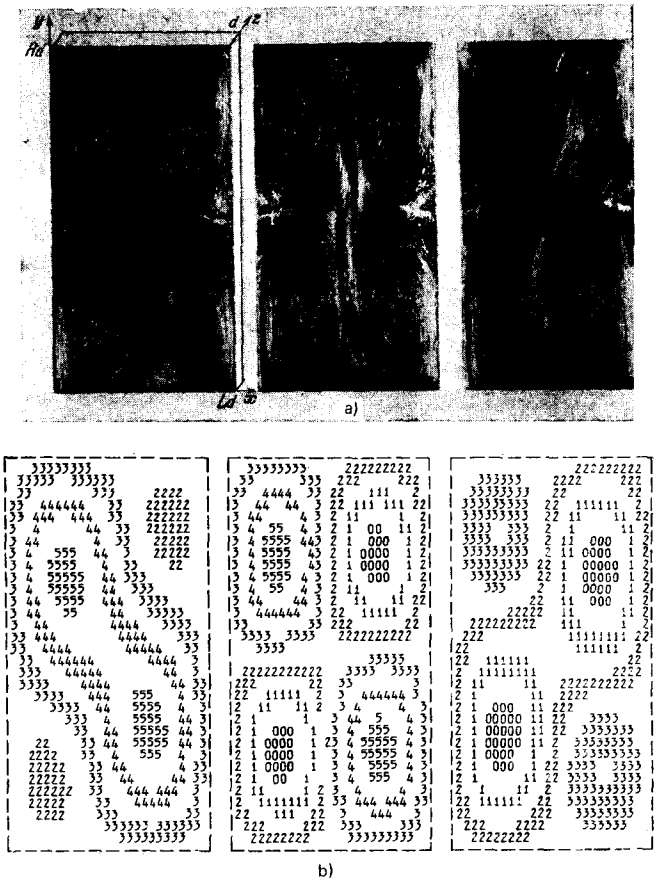

FIG. 26. Experimental (a) and simulated (b) flow lines in a Hele-Shaw cell at different times.

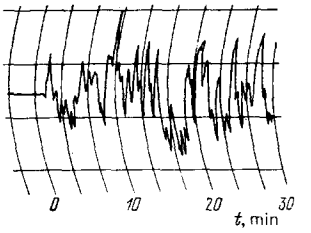

FIG. 27. Output of a thermocouple placed at the central section of a Hele-Shaw cell (stochastic regime).

In the experiments described by Lyubimov *et al.*,[81] a constant temperature gradient G independent of the rate of motion within the gap was maintained on the wide solid walls of the cell. In a number of experiments, one of the wide walls was transparent, so that it was possible to observe the change in motion as **Ra** was increased. Stationary single-vortex convective motion was found to appear for $\mathbf{Ra}>\mathbf{Ra}_{\mathrm{I}}$ and persisted up to $\mathbf{Ra}=\mathbf{Ra}_{\mathrm{II}}$. Further increase in the Rayleigh number (i.e., in the vertical temperature gradient) led to the appearance of stationary two- or four-vortex convection for $\mathbf{Ra}>\mathbf{Ra}_{\mathrm{II}}$. Stationary cellular convection was then replaced at higher values of **Ra** by a dynamic oscillatory regime. The next transition led to the establishment (for $\mathbf{Ra}>\mathbf{Ra}_{\mathrm{I}}$) of irregular vortex motion with the characteristic random paired linking of the vortices. Figure 27 shows the pulsations of the temperature difference within the cell corresponding to this turbulent regime.

The model used to explain all the experimentally observed transitions was a natural generalization (or, more precisely, extension) of the Lorenz model. The equations of free convection in the Boussinesq approximation had the form

$$\left.\begin{aligned}&\frac{\partial \mathbf{v}}{\partial t}+(\mathbf{v}\nabla)\,\mathbf{v}=-\frac{\nabla p}{\rho_0}+\nu\Delta\mathbf{v}-\mathbf{g}\beta T,\\&\frac{\partial T}{\partial t}+(\mathbf{v}\nabla)\,T=\varkappa\Delta T,\\&\operatorname{div}\mathbf{v}=0\end{aligned}\right\}\tag{3.3}$$

(same notation as before). Assuming that the flow structure along z is given, we can introduce the flow function ψ such that $v_x=-\partial\psi/\partial y$, $v_y=\partial\psi/\partial x$. In terms of the dimensionless variables $x=x_0/d$, $t=(\varkappa/d^2)t_0$, $\theta=(T/d)G$, $\psi=\psi_0/\varkappa$, the original equations take the form

$$\left.\begin{aligned}&\frac{1}{\mathrm{Pr}}[\omega_t+J(\psi,\omega)]=\Delta\omega+\mathrm{Ra}\,\theta_x,\\&\theta_t+J(\psi,\theta)=\Delta\theta+\psi_x,\end{aligned}\right\}\tag{3.4}$$

where $\omega=-\psi_{xx}-\psi_{yy}$ is the vorticity, θ is the departure of the temperature from the equilibrium value, $\mathbf{Ra}=g\beta Gd^4/\nu\varkappa$ is the Rayleigh number, and J is the Jacobian. The next step is to seek the general solution in the form

$$\left.\begin{aligned}&\psi=\sum\psi_{nm}(t)\sin\frac{n\pi}{L}x\cdot\sin\frac{m\pi}{H}y\cdot\cos\frac{\pi}{2}z,\\&\theta=\sum\theta_{nm}(t)\cos\frac{n\pi}{L}x\cdot\sin\frac{m\pi}{H}y\cdot\cos\frac{\pi}{2}z,\end{aligned}\right\}\tag{3.5}$$

where H and L are, respectively, the dimensionless vertical and horizontal dimensions of the cell (in this particular experiment, $H=20$ and $L=10$). These are then used to obtain equations of the form of (3.2) for ψ_{nm}, θ_{nm} with $f_k=0$.

The trivial solution of this system, $\psi_{nm}=\theta_{nm}=0$, corresponds to the mechanical equilibrium which is stable for

$$\mathbf{Ra}<\mathbf{Ra}_0=\pi^4\left[1+\left(\frac{L}{H}\right)^2\right]\left(\frac{1}{L^2}+\frac{1}{H^2}+\frac{1}{4}\right).\tag{3.6}$$

For $\mathbf{Ra}>\mathbf{Ra}_0$, we have stationary single-cell convection, i.e., the modes ψ_{11}, θ_{11}, and θ_{02} differ from zero, and all the others are not excited, as before. The set of equations for these modes is the same as the well-known Lorenz system. In principle, the turbulent regime could have appeared even for this monocellular convection if the critical Rayleigh number $\mathbf{Ra}_T$[35] could be exceeded within the stable single-vortex regime. However, the stochasticity described by the Lorenz system does not have time to appear, i.e., the modes ψ_{22}, θ_{22}, ψ_{31}, θ_{31}, θ_{04} appear much earlier for $\mathbf{Ra}=\mathbf{Ra}_c<\mathbf{Ra}_T$, and three- or four-cell convection is established. The set of equations for these modes takes the form of three coupled Lorenz systems of the form: ($\psi_{11}\sim X_1$, $\theta_{11}\sim Y_1$, $\theta_{02}\sim Z_1$, $\psi_{31}\sim X_2$, $\theta_{31}\sim Y_2$, $\theta_{04}\sim Z_2$, $\psi_{22}\sim X_3$, $\theta_{22}\sim Y_3$)[36]

[35] It is precisely this situation that occurs in the convective loop.[89]

[36] For clarity, positive coefficients are omitted from (3.7).

$\theta_{22} \sim Y_3$) *):

$$\left.\begin{aligned}
\dot{X}_1 &= \boxed{Y_1 - X_1} \quad \boxed{+X_2X_3}, \\
\dot{Y}_1 &= \boxed{X_1 - Y_1 - Y_1Z_1} \quad \boxed{+Y_2X_3 + Y_3X_2}, \\
\dot{Z}_1 &= \boxed{-Z_1 + X_2Y_2} \quad \boxed{-Z_1 + X_1Y_1}, \\
\dot{X}_2 &= \boxed{Y_2 - X_2} \quad \boxed{+X_1X_3}, \\
\dot{Y}_2 &= \boxed{X_2 - Y_2 - X_2Z_1} \quad \boxed{-Y_1X_3 + Y_3X_1}, \\
\dot{Z}_2 &= \boxed{-Z_2 + X_3Y_3}, \\
\dot{X}_3 &= \boxed{Y_3 - X_3} \quad \boxed{-X_1X_2}, \\
\dot{Y}_3 &= \boxed{X_3 - Y_3 - X_3Z_2} \quad \boxed{-Y_1X_2 - Y_2X_1}.
\end{aligned}\right\} \tag{3.7}$$

This system was investigated numerically. It was found that regular oscillations (limit cycle in the phase space of (3.7)) became established for $\mathbf{Ra} > \mathbf{Ra}_c$ in a narrow range of **Ra**, the amplitude of these oscillations increased monotonically with increasing **Ra**, and this was followed by the stochastic regime. The agreement between the numerical and the experimental results was exceedingly convincing. In particular, the values of the Rayleigh number for which stationary ($\mathbf{Ra}_0$), regular oscillatory ($\mathbf{Ra}_c$), and turbulent ($\mathbf{Ra}_T$) motions became established were found to agree with the calculated results to within 5%! Figure 26 shows the experimental and calculated flow lines corresponding to the same parameter values.

We emphasize one exceedingly important point. If the initial conditions differed from zero for a large number of modes in (3.5), then a complex transient process would be followed by the damping of modes without symmetry (for example, ψ_{12}, ψ_{21}, θ_{12}, θ_{21}, θ_{01}, etc.), and the behavior of the other modes would be independent of the initial conditions.

The Lorenz equations provide us with an elementary building block for constructing many systems of hydrodynamic type describing different convective motions. In particular, Lorenz himself succeeded in describing turbulent flows, observed in experiments on the convection of a liquid in the interior of a rotating cylindrical channel, with the aid of 14 equations. An analogous convection model was constructed by Dolzhanskiĭ and Pleshanov for an ellipsoid heated from below. They investigated a model of six equations, i.e., two coupled Lorenz systems[80]:

$$\left.\begin{aligned}
\dot{\Omega}_1 &= -\frac{I_3 - I_2}{I_1}\Omega_2\Omega_3 - \sigma\Omega_1 + \frac{I_2}{I_1}\sigma\theta_2, \\
\dot{\Omega}_2 &= +\frac{I_3 - I_1}{I_2}\Omega_1\Omega_3 - \sigma\Omega_2 + \sigma\theta_1, \\
\dot{\Omega}_3 &= -\frac{I_2 - I_1}{I_3}\Omega_1\Omega_2 - \sigma\Omega_3, \\
\dot{\theta}_1 &= -\Omega_2\theta_3 - \Omega_3\theta_2 + r\Omega_2 - \theta_1, \\
\dot{\theta}_2 &= \Omega_3\theta_1 - \Omega_1\theta_3 + r\Omega_1 - \theta_2, \\
\dot{\theta}_3 &= \Omega_1\theta_2 + \Omega_2\theta_1 - \theta_3;
\end{aligned}\right\} \tag{3.8}$$

where Ω_j and θ_j are proportional to the components of the angular velocity of the liquid and of the gradient of the deviation of the temperature from the equilibrium value, taken along the principal axes of the ellipsoid, and $\sigma \sim \mathbf{Pr}$, $r \sim \mathbf{Ra}$. The minor axis of the ellipse (x_3) is parallel to the gravitational field and $I_3 > I_2 > I_1$. In the absence of heating, $\theta_{1,2,3} = 0$, and (3.8) describes damped oscillations of a "liquid top." Stable three-mode motions are absent when heating is introduced and, in particular, even the Lorenz attractor which appears for $\Omega_1 = \theta_2 = \Omega_3 = 0$ (or $\theta_1 = \Omega_2 = \Omega_3 = 0$) is unstable for $r = 17$ (when $\sigma = 6$). Both the barotropic and baroclinic mechanisms of instability can be simultaneously analyzed within the framework of this model.[37)] It was found that the appearance of additional, barotropic, instability may suppress the stochasticity present in the three-mode model by converting the motion into a regular motion.

As we have seen, stochastic behavior may appear in a dissipative system containing only three modes. However, this stochastic behavior can only have a qualitative relation to real turbulence (as a mechanism responsible for the appearance of disorder). The question is—how many modes are necessary to achieve a quantitative description of the transition to turbulence? For example, in the analysis of the convective loop, three modes are sufficient (single-vortex motion.[89] In the Hele-Shaw cell, turbulent convection appears on the "basis" of 8–9 modes. To produce the transitions to turbulence, Martin and McLaughlin[46] needed 39 modes in the case of a layer heated from below. For $\mathbf{Pr} = 1$, they observed the following transitions:

(1) for $r = \mathbf{Ra}/\mathbf{Ra}_I = 1.25$—stationary convection;
(2) for $1.25 < r < 1.45$—periodic regime;
(3) for $1.45 < r < 1.5$—weak stochasticity;
(4) for $1.5 < r < 1.6$—again a periodic regime, and
(5) for $r > 1.6$—developed stochasticity.

These transitions, with the exception of (3), correspond to actually observed situations for small Prandtl numbers (Fig. 22).

One can assert that the number of modes on which turbulence is based depends on the geometry of the problem and on the nature of the instability, i.e., on the form of the neutral curve. Indeed, the convective loop is essentially a one-dimensional resonator with a very depleted spectrum, the Hele-Shaw cell is a two-dimensional resonator, and the flat layer heated from below can support both two-dimensional (whose growth rate increases quite rapidly with increasing **Ra**) and three-dimensional disturbances. These disturbances were first taken into account by Lorenz,[90] McLaughlin and Martin,[46] and Gertsenshteĭn and Shmidt[84,99] in connection with describing turbulent thermal convection in a layer. A stochastic convection regime in a rotating layer was discovered in the latter papers.

[37)] Baroclinic instability, typical for thermal convection, is connected with the interaction between the velocity and temperature modes; barotropic instability is connected with the interaction between different velocity modes. This instability is determined by the special geometry of the cavity and, in particular, the barotropic mechanism can be excluded by using a spherical cavity.

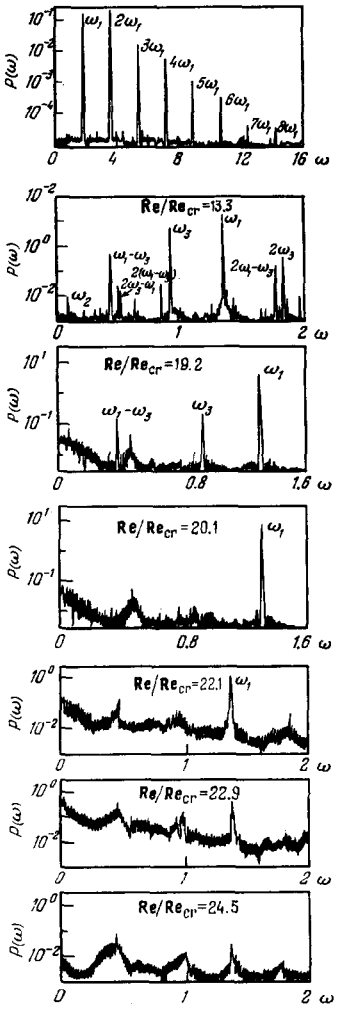

FIG. 28. Experimental results on the transition to turbulence in Couette flow between cylinders.[102] The Reynolds number is normalized to the critical value corresponding to the onset of Taylor vortices.

h) Transition to turbulence in Coutte flow between cylinders

Quite recently, Gollub *et al.*[85,102] investigated the appearance of turbulence in Couette flow produced when the inner cylinder is rotated. A laser beam and the Doppler effect were used to measure the radial velocity component V_r of the fluid. Polystyrene spheres, 4.8×10^{-5} cm in diameter, were introduced into the water to increase the precision of the experiment. The measured function $V_r(t)$ was then used to determine the power spectrum and hence to identify the various transitions. No change in the spatial structure of the flow could be detected for any of the observed transitions (after the appearance of azimuthal waves). The number of vortices along the vertical was 17 and the number of waves along the azimuth remained equal to four. The 17/4 state having been attained remained stable for $2<\mathrm{Re/Re}_{cr}<45$, where Re_{cr} is the value of Re for which Taylor vortices appear and V_r becomes a periodic function of z. The fact that the apparent structure of the flow and the rotational couple remained constant during the observed transitions explains why these transitions were not noted in previous experiments. The evolution of the power spectrum of the pulsations of $V_r(t)$ during the transitions can be seen in Fig. 28: (1) Taylor vortices appeared for $\mathrm{Re}>\mathrm{Re}_{cr}$; the intensity of the pulsations grew with increasing Re near the transition, in accordance with the Landau expression $\sqrt{\mathrm{Re}-\mathrm{Re}_{cr}}$; for larger Re, when the correction due to the next approximation had to be introduced, the dependence was of the form $(\mathrm{R}-\mathrm{R}_{cr})^{3/2}$, which was first introduced by Davey[105]; (2) for $\mathrm{Re/Re}_{cr}=1.3$, there was a periodic azimuthal wave of frequency ω_1 with $m=4$ (see Fig. 28, where all the frequencies are normalized to the rotational frequency of the inner cylinder); (3) a low-frequency spectral component at $\omega_2=0.2$ was noted in some of the experiments as Re was increased (it is possible that this was connected with the modulation instability of the Taylor vortices[102,73]); (4) for $\mathrm{Re/Re}_{cr}=10.0\pm0.2$, the discrete component at $\omega_3=(2/3.3)\omega_1$ and the components at the combination frequencies $\omega_1-\omega_3$, $2\omega_3-\omega_1$, $\omega_1-(2\omega_3-\omega_1)$, and $2\omega_1-\omega_3$ appeared softly without hysteresis (they are shown in Fig. 28 for $\mathrm{Re/Re}_{cr}=13.3$; (5) as Re was increased, the amplitude of ω_3 and together with it the amplitudes of the combination components were found to fall and, for $\mathrm{Re/Re}_{cr}=19.8\pm0.1$, all the discrete components other than ω_1 disappeared, but the diffuse peak at $\omega\approx\omega_1/3$, which first appeared for $\mathrm{Re/Re}_{cr}=17$ was found to persist. The separation between ω_1 and ω_3 was found to decrease continuously with increasing Re: when $\mathrm{Re/Re}_{cr}=10.0$, the ratio ω_1/ω_3 was 1.63 whereas, for $\mathrm{Re/Re}_{cr}=19.8$, it was 1.41; (6) finally, the last of the remaining discrete components ω_1 vanished for $\mathrm{Re/Re}_{cr}=22.4\pm0.2$, and the flow was transformed from quasiperiodic to random and was characterized by a continuous spectrum with a decreasing autocorrelation function (Fig. 29). The flow was investigated up to $\mathrm{Re/Re}_{cr}=45$ and no further transitions were observed. The width of the discrete peaks was $\Delta\omega\approx0.001$ and the frequency ω_1 was equal to that found by Coles.[73] The authors of the experiment also emphasized that, after the transition to turbulence, the spectrum still contained diffuse peaks at frequencies that were multiples of $\omega_1/3$.

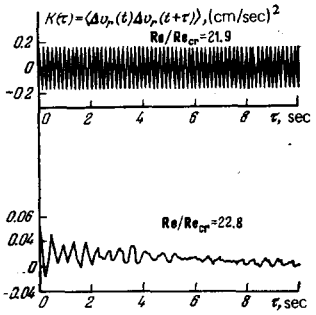

FIG. 29. Autocorrelation function for velocity, before and after the disappearance of the discrete spectral component (at $\mathrm{Re/Re}_{cr}=22.4$).

The fact that the appearance of the continuous spectrum is, in this case, connected not with the appearance of a large number of incommensurable frequencies but, on the contrary, with the vanishing of narrow discrete components and the appearance of diffuse

peaks, suggests that the observed transition to turbulence could be described within the framework of the finite-dimensional model. For a detailed description of all the transitions,[38] the number of modes in this model must not be too small. Without attempting to simulate all the observed transitions, let us consider the single most important transition, i.e., the sudden transformation of the discrete component ω_1 into a diffuse peak. Using the fact that, immediately before the transition, the spectrum contains not only ω_1 but also the diffuse peaks at $\omega_1/3$ and $(2/3)\omega_1$,[39] we can simulate the transition by the simplest model, namely, three resonantly coupled quasiharmonic (in time) modes with frequencies ω_1, $(2/3)\omega_1$, and $\omega_1/3$. The equations for the complex amplitudes a_3, a_2, and a_1 of these modes are

$$\left.\begin{aligned}\dot{a}_3&=\gamma a_3-3a_1a_2-\rho|a_3|^2a_3,\\ \dot{a}_2&=\varkappa a_2-a_1^2+2a_1^*a_3-\rho|a_2|^2a_2,\\ \dot{a}_1&=-\nu a_1+a_2a_1^*+a_3a_2^*.\end{aligned}\right\} \tag{3.9}$$

Here, the quadratic components describe the resonant interaction between the modes due to the quadratic hydrodynamic nonlinearity and the cubic terms represent the nonlinear damping connected with self-interaction and the transfer of energy to the damped harmonics; $\gamma>0$ characterizes the growth rate of the main mode ω_1 and $\nu>0$ the damping at $\omega_1/3$. The parameter $\varkappa$ can be either positive or negative.

The transfer of energy from the intensively growing mode ω_1 to the subharmonics, which is described by (3.9), has been investigated numerically.[86,106] It was found that the transfer of energy down the spectrum in this decay process (for different values of the coefficients γ, $\varkappa$, and ν) could be stationary [stable equilibrium in the phase space of (3.9)], periodically modulated (stable limit cycle in phase space), and randomly modulated [the solution of (3.9) is then characterized by a continuous spectrum and a falling autocorrelation function]. This is illustrated in Fig. 30. Since we are concerned with quasiharmonic processes, the transition from the dynamic to the stochastic process corresponds to the transformation of the discrete components into diffuse peaks in the spectrum of the (velocity) fields themselves. The fact that the components $\omega_1/3$ and $(2/3)\omega_1$ were broadened even before the transition should apparently have no qualitative effect on the appearance of stochasticity which is described within the framework of (3.9), including the case when $\varkappa<0$.

i) The role of decays in the appearance of turbulence

As we have just seen, decays, i.e., the transfer of energy from the growing high-frequency perturbations

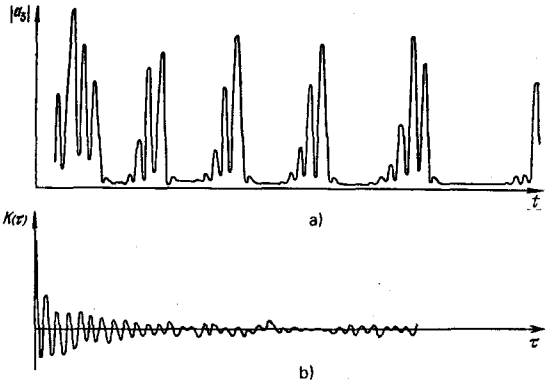

FIG. 30. Realization (*a*) and its correlation function (*b*) obtained by numerical analysis of the model given by (3.9) with $\rho=0.2$.

downward along the spectrum (this was discussed in detail in Sec. 2), play an important role in the appearance of turbulence, in thermal convection, and in Couette flow. It would appear that the decay mechanism for generating disorder, which is quite common for self-oscillatory systems, is directly related to the nature of hydrodynamic turbulence near its onset.

This is also confirmed by experiments on transitions to turbulence in a wake.[87,88] Sato[87] has investigated the onset of turbulence in a symmetric flow with a velocity gradient and found that the presence of disturbances at frequencies f_1 and f_2 was accompanied by the effective transfer of energy to the mode with the difference frequency f_2-f_1 which, in turn, was accompanied by the randomization of these low-frequency oscillations. Analogous results have been obtained by Miksad,[88] who analyzed the transition to turbulence in plane-parallel flow. The flow was subjected to perturbations at the frequency corresponding to the maximum growth rate. The leading effect observed in this situation was the generation of a subharmonic and the strong "noise" broadening of the spectrum (Fig. 31).

Subharmonic generation, which precedes the onset of turbulence, was also observed in the numerical simulations of Gertsenshtein *et al.*,[62] who simulated the wake by a piecewise-linear velocity profile, and, in recent boundary-layer experiments by Kachanov *et al.*[103] They investigated the evolution of the Tollmien-Schlichting waves of finite amplitude on a plate. The experiments were performed in a wind tunnel with a very low level of natural turbulence (0.04%), so that very fine features of preturbulence could be examined. It was found that, near the transition to turbulence, the growth of the main wave and of its harmonics was initially stabilized. Their amplitudes were then found to fall, but this was accompanied by an increase in the level of low-frequency pulsations

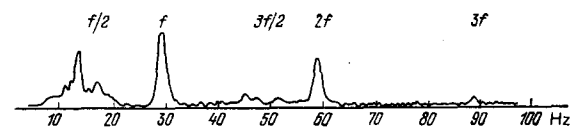

FIG. 31. Pulsation spectrum in the sheared layer.[87]

[38] The first transitions, i.e., the appearance of the Taylor vortices and periodic azimuthal waves, are satisfactorily explained within the framework of the simple "nonresonance" model such as (2.1). This explanation was first given by Stuart.[71]

[39] The smearing out of the peaks at these frequencies can be connected, for example, with the enhancement of the role of fluctuations near the bifurcation, which corresponds to the vanishing of the growth rate at frequence ω_3.

which should have been damped out according to the linear theory. In all the experiments, the spectrum of these pulsations contains a peak at half the frequency of the main wave. This peak broadens and then vanishes as the Reynolds number increases. The same experiment shows the presence of a low-frequency component in the spectrum, whose frequency is very dependent on the amplitude of the main wave. It may be that pulsations of this frequency appear as a result of decay processes of higher order and correspond, for example, to the modulation instability of the Tollmien-Schlichting waves.

CONCLUSIONS

1. The appearance of stochasticity in dissipative systems (and, indeed, in conservative systems) has, until recently, been intuitively related only to the excitation in a given system of a very large number of degrees of freedom. Indeed, any particular motion of a system of, say, 10^{23} modes (or molecules) can be reproduced experimentally only in principle. In practice, motion of this kind is not reproducible if only because it is impossible to specify more than once the same initial conditions for such a large number of particles.[40] However, it is now clear that there are dissipative systems with a small number of degrees of freedom whose behavior is equally unreproducible (when the initial conditions are specified with arbitrarily high but, nevertheless, finite precision). The reason for this lies in the unstability (divergence) and the tangling of paths within the attractor, i.e., an attractive region in the phase space of the system. The existence of the so-called strange attractors in the phase space of very different physical (and not only physical[26,31,91,92,96]) systems has turned out to be almost as common as, for example, the existence of limit cycles.

2. From the point of view of the average description of a system with strange attractors, it is exceedingly interesting to find the statistics of the behavior of the system from the known structure of the strange attractor. It is possible that the most natural way will be to transform from phase flows to mappings, and to use the symbolic description. However, even for the popular Lorenz system, this problem is still in the initial stage of solution.[51,52,54,109]

3. A very important point in connection with the above problem is that the small fluctuations present in any physical system cannot destroy a strange attractor. Moreover, they apparently have very little effect on the statistics of the system "characterized by a strange attractor," i.e., the exponential divergence of paths within the attractor turns out to be "more important" than a random external force.[95]

4. Turbulence, i.e., stochastic self-oscillations of a continuous medium or field, is connected with the instability of solutions not of ordinary but of partial differential equations. It is therefore natural that the strange attractor is a representation of only the type of turbulence that admits of a finite-dimensional representation. In hydrodynamics, this is valid, for example, for two-dimensional flows or for the motion of a liquid or gas in a bounded cavity (resonator). Here, we have, in particular, the remarkable experiment with the Hele-Shaw cell which confirms the "attractor" model of turbulence in the case of thermal convection.

5. The fact that the strange attractor is the direct mapping of "finite-dimensional" turbulence that is characterized by a continuous spectrum in time but is discrete in space, is currently only one aspect—clearer than the others—of its connection with the theory of turbulence. It is possible that the role of strange attractors in the theory of stochastic self-oscillations of distributed systems and in the theory of hydrodynamic turbulence is, in particular, broader and is similar to the role of periodic or solitary stationary waves in the theory of regular self-oscillations. Thus, a nonequilibrium dissipative medium can, in principle, support "random" stationary waves which correspond to the strange attractor in the phase space of the system describing the stationary (or other self-preserving) motions. However, research in this area is only just beginning and, as yet, we know of no specific results.

The author is indebted to A. A. Andronov, A. V. Gaponov, V. R. Kogan, O. A. Ladyzhenskaya, A. S. Pikovskiĭ, Ya. G. Sinaĭ, A. L. Fabrikant, and V. I. Yudovich for numerous fruitful discussions and suggestions, and to A. S. Pikovskiĭ for major assistance in the preparation of this review.

[40] Whether an ensemble of a large number of modes will exhibit a dynamic or statistical behavior will, of course, depend not only on the number of modes but also on the nature of the coupling between them. Stationary nonlinear waves in a continuous medium are an example of the dynamic behavior of a system consisting of an infinite number of modes. In media with dispersion, such waves are the result of mutual frequency locking of an infinite number of spatial harmonics.

[41] This list of references is not meant to be complete. In particular, it does not reflect the content of the many mathematical papers that are listed elsewhere.[17,19,23] Recent work in this area is described in the literature.[111,112]

[1] R. P. Feynman, R. B. Leighton, and M. Sands, Feynman Lectures on Physics, A. W., An Arbor, USA (Russ. Transl., Mir, M., 1967).
[2] A. A. Andronov, *Sobranie trudov (Collected works)*, Izd. AN SSSR, M., 1956.
[3] S. M. Rytov, Usp. Fiz. Nauk **62**, 493 (1971) [*sic*].
[4] L. D. Landau, Dokl. Akad. Nauk SSSR **44**, 339 (1944).
[5] L. D. Landau and E. M. Lifshitz, Mekhanika sploshnykh sred (*Mechanics of Continuous Media*), Gostekhizdat, M., 1953 (English Transl., Pergamon Press, Oxford, 1975).
[6] E. Hopf, Comm. Pure and Appl. Math. **1**, 303 (1948).
[7] V. I. Arnol'd, Matematicheskie metody klassicheskoĭ mekhaniki (Mathematical Methods in Classical Mechanics), Nauka, M., 1974.
[8] P. C. Hemmer L. C. Maximon, and H. Wergeland, Phys. Rev. **111**, 689 (1958).
[9] S. Chandrasekhar, Stochastic Problems in Physics and As-

tronomy (Russ. Transl., IL, M., 1947).
[10]D. Ruelle and F. Takens, Comm. Math. Phys. **20**, 167 (1971).
[11]N. S. Krylov, Raboty po obosnovaniyu statisticheskoĭ fiziki (Papers on the Foundations of Statistical Physics), Izd. AN SSSR, M.-L., 1950.
[12]M. Born, Usp. Fiz. Nauk **69**, 2 (1959).
[13]G. M. Zaslavskiĭ, Statisticheskaya neobratimost' v nelineĭnykh sistemakh (Statistical Irreversibility in Nonlinear Systems), Nauka, M., 1970.
[14]G. M. Zaslavskiĭ and B. V. Chirikov, Usp. Fiz. Nauk **105**, 3 (1971) [Sov. Phys. Usp. **14**, 549 (1972)].
[15]E. Hopf, Usp. Mat. Nauk **4** (1), 113 (1949).
[16]D. V. Anosov, Dokl. Akad. Nauk SSSR **151**, 1250 (1963) [*sic*].
[17]D. V. Anosov, Geodizicheskie potoki na kompaktnykh rimanovykh mnogoobraziyakh otritsatel'noĭ krivizny (Geodesic Flows on Compact Riemannian manifolds of Negative Curvature (Abstract MIAN SSSR), Vol. 90, Nauka, M., 1967.
[18]Ya. G. Sinaĭ, Lektsii po statisticheskoĭ teorii (Lectures on Statistical Theory), Erevan State University, 1975.
[19]S. Smale, Bull. Am. Math. Soc. **73**, 747 (1967) (Russ. Transl., Usp. Mat. Nauk **25**, 113 (1970)).
[20]V. M. Alekseev, A. B. Katok, and A. G. Kushnerenko, Gladkie dinamicheskie sistemy, in IX letnyaya matematicheskaya shkola, Kiev. (Smooth Dynamic Systems, in: Ninth Summer Mathematical School, Kiev), Institute of Mathematics, Ukrainian Academy of Sciences, 1972.
[21]Z. Nitecki, Differentiable Dynamics: An Introduction to the Orbit Structure of Diffeomorphisms, MIT Press, 1971 (Russ. Transl. Mir, M., 1975).
[22]J. Moser, Stable and Random Motions in Dynamical Systems, Princeton, N.J., 1973.
[23]V. M. Alekseev, Simvolicheskaya dinamika, in XI letnyaya matematicheskaya shkola, Kiev (Symbolic Dynamics, in: Eleventh Summer Mathematical School, Kiev), Institute of Mathematics, Ukrainian Academy of Sciences, 1976.
[24]Ya. G. Sinaĭ, in Nelineĭnye volny (in: Nonlinear Waves), ed. by A. V. Gaponov, Nauka, M., 1978.
[25]M. Henon and C. Heiles, Astron. J. **69**, 73 (1964).
[26]O. E. Rössler, Z. Naturforsch. Teil A **31**, 259 (1976).
[27]A. S. Pikovskiĭ and M. I. Rabinovich, Dokl. Aka. Nauk SSSR **239**, 314 (1978) [*sic*].
[28]A. A. Kosyakin and E. A. Sandler, Izv. Vyssh. Uchebn. Zaved. Ser. Mat. **3**, 32 (1972).
[29]A. N. Sharkovskiĭ, UMZh. **16**, 61 (1964).
[30]T. Y. Li and J. A. Yorke, Am. Math. Monthly **82**, 985 (1975).
[31]R. M. May, Nature **262**, 459 (1976).
[32]P. Billingsley, Ergodic Theory and Information, John Wiley, New York (1965) (Russ. Transl., Mir, M., 1969).
[33]Ya. G. Sinaĭ, Usp. Mat. Nauk **27**, 21 (1972).
[34]L. Brillouin, Science and Information Theory, 2nd ed., Academic Press, New York, 1962 (Russ. Transl. of earlier ed., Fixmatgiz, M., 1960).
[35]E. Lorenz, J. Atmos. Sci. **20**, 130 (1963).
[36]Van Danzig, Fund. Math. **15**, 102 (1930).
[37]R. V. Plykin, Matem. Sb **94** (136), 143 (1974).
[38]M. I. Rabinovich, Izv. Vyssh. Uchebn. Zaved. Radiofiz. **17**, 477 (1974).
[39]Y. Aizawa, Prog. Theor. Phys. **56**, 703 (1976).
[40]S. Ya. Vyshkind and M. I. Rabinovich, Zh. Eksp. Teor. Fiz. **72**, 557 (1976) [Sov. Phys. JETP **44**, 292 (1976)].
[41]S. Ya. Vyshkind, M. I. Rabinovich, and A. L. Fabrikant, Izv. Vyssh. Uchebn. Zaved. Radiofiz. **20**, 2 (1977).
[42]V. I. Dubrovin, V. R. Kogan, and M. I. Rabinovich, Fiz. Plazmy **4**, 920 (1978) [Sov. J. Plasma Phys. **4**, 514 (1978)].
[43]A. S. Pikovskiĭ, M. I. Rabinovich, and V. Yu. Trakhtengerts, Zh. Eksp. Teor. Fiz. **74**, 1366 (1978) [Sov. Phys. JETP **47**, 715 (1978)].
[44]H. Haken, Phys. Lett. A **53**, 77 (1975).
[45]R. Graham, Phys. Lett. A **58**, 440 (1976).
[46]J. B. McLaughlin and P. C. Martin, Phys. Rev. **A12**, 186 (1975).
[47]O. Lanford, Preprint, 1976.
[48]V. S. Afraĭmovich, V. V. Bykov, and L. P. Shil'nikov, Dokl. Akad. Nauk SSSR **234**, 336 (1977) [Sov. Phys. Dokl. **22**, 253 (1977)].
[49]E. B. Vul and Ya. G. Sinaĭ, in Mnogokomponentnye sluchaĭnye sistemy (Multicomponent Random Systems), Nauka, M., 1978.
[50]J. Guckenheimer, J. E. Marsden, and M. McCracen, in: The Hopf Bifurcation and Its Applications, Springer-Verlag, N.Y., 1976, p. 368.
[51]R. F. Williams, Preprint, 1976.
[52]J. Guckenheimer, Preprint, 1976.
[53]L. P. Shil'nikov, Matem. Sb. **76** (116), 378 (1967).
[54]M. Lucke, J. Stat. Phys. **15**, 455 (1976).
[55]A. V. Gaponov, M. I. Rabinovich, and M. F. Shapiro, Vestn. Mosk. Univ. Fiz. Astron. No. 4, 42 (1978).
[56]Ya. I. Khanin, Dinamika kvantovykh generatorov (Dynamics of Quantum Mechanical Generators), Sovet-skoe Radio, M., 1975.
[57]B. B. Kadomtsev and V. I. Karpman, Usp. Fiz. Nauk **103**, 193 (1971).
[58]K. Yakobs, in: Turing Machines (Topics in Pure Mathematics), Harper and Row, Scranton, PA [Sov. Phys. Usp. **14**, 40 (1972)] (Russ. Transl., Mir. M., 1972).
[59]Yu. I. Neĭmark, Metod tochechnykh otobrazheniĭ v teorii nelineĭnykh kolebaniĭ (Point Mapping in the Theory of Nonlinear Oscillations), Nauka, M., 1972.
[60]V. V. Papko, M. I. Rabinovich, and A. Yu. Sokolov, Pis'ma Zh. Tekh. Fiz. **3**, 436 (1977) [Sov. Tech. Phys. Lett. **3**, 176 (1977)].
[61]I. I. Blekhman, Sinkhronizatsiya dinamicheskikh sistem (Synchronization of Dynamic Systems) Nauka, M., 1971.
[62]S. Ya. Gertsenshteĭn, A. N. Sukhorukov, and V. Ya. Shkadov, Izv. Akad. Nauk SSSR Ser. Mekhanika Zhidkosti i Gaza No. 3, 10 (1977).
[63]O. A. Ladyzhenskaya, Zap. Nauch. Seminarov LO MIAN SSSR (Leningrad Branch, Acad. Sci. USSR) No. 27, 91, 1972, "Nauka", L.
[64]R. Tom, SIAM Rev. **19**, 189 (1977).
[65]P. C. Martin, J. Phys. (Paris) **37**, 57 (1976).
[66]G. Z. Gershuni and E. M. Zhukovitskiĭ, Konvektivnaya ustoichivost' neszhimaemoĭ zhidkosti (Convective Stability of Incompressible Fluids), Nauka, M., 1972.
[67]R. Krishnamurti, J. Fluid Mech. **60**, 285 (1973).
[68]T. Y. Chy and R. J. Goldstein, J. Fluid Mech. **60**, 285 (1973).
[69]D. C. Threlfall, J. Fluid Mech. **67**, 17 (1975).
[70]G. Ahlers, Phys. Rev. Lett. **33**, 1185 (1974).
[71]J. T. Stuart, in: Fluid Dynamics Transactions, Vol. 5, Inst. of Fundamental Techn. Research, Polish Academy of Sciences, Warsaw, Part 1.
[72]G. I. Taylor, Philos. Trans. R. Soc. London Ser. A **223**, 285 (1923).
[73]D. Coles, J. Fluid Mech. 21(Part 3), 385 (1965).
[74]A. S. Monin and A. M. Yaglom, Statisticheskaya gidromekhanika (Statistical Hydromechanics), Nauka, M., 1965, Part 1 (English Trans., Statistical Fluid Mechanics: Mechanics of Turbulence, MIT Press, 1975).
[75]H. Schlichting and K. Schlichting, Boundary Layer Theory, 6th. ed. McGraw-Hill, New York, 1968 (Russ. Transl., Mir, M., 1974).
[76]R. Betchov and W. O. Criminale, Stability of Parallel Flows, Academic Press, 1967 (Russ. Transl., Mir, M., 1971).
[77]L. da Vinci, Selected Papers on Natural Philosophy (Russ. Transl., Izd. AN SSSR, M., 1955).
[78]T. von Karman, Phys. Z. **13**, 49 (1912).
[79]Y. V. Chen, Schweizerische Bauzeitung **13**, 49 (1972); **91**, 1049 (1973).
[80]F. V. Dolzhanskiĭ, V. I. Klyatskin, A. M. Obukhov, and M. A. Chusov, Nelineĭnye sistemy gidrodinamicheskogo tipa (Nonlinear Systems of the Hydrodynamic Type), Nauka, M., 1974.
[81]D. V. Lyubimov, G. F. Putin, and V. I. Chernatynskiĭ. Dokl. Akad. Nauk SSSR **234**, 534 (1977) [Sov. Phys. Dokl. **22**, 360 (1977)].

[82]Turbulence Seminar (Lecture Notes in Mathematics, No. 615), Springer-Verlag, N. Y., 1977.
[83]L. I. Mandel'shtam, Sobranie trudov (Collected Papers), Vol. 2, Izd. AN SSSR, M., 1947, p. 13.
[84]S. Ya. Gertsenshteĭn and V. M. Shmidt, Izv. Akad. Nauk SSSR Ser. Mekhanika Zhidkosti i Gaza No. 2, 9 (1977).
[85]J. P. Gollub and H. L. Swinney, Phys. Rev. Lett. **35**, 927 (1975).
[86]M. I. Rabinovich, A. G. Sazontov, and A. L. Fabrikant, in Teoriya difraktsii i rasprostraneniya voln. Teksty dokladov (The Theory of Diffraction and Wave Propagation, Text of Papers), Vol. 1, Oceanographic Commission of the USSR Academy of Sciences, M., 1977, p. 25.
[87]H. Sato, J. Fluid Mech. **44**, 741 (1970).
[88]R. W. Miksad, J. Fluid Mech. **56**, 695 (1972); **59**, 1 (1973).
[89]H. F. Creveling *et al.*, J. Fluid Mech. **67**, 65 (1975).
[90]E. Lorenz, J. Atmos. Sci. **30**, 448 (1963).
[91]O. E. Rossler, Phys. Lett. A **57**, 397 (1976).
[92]O. E. Rossler, Z. Naturforsch. Teil A **31**, 1168 (1976).
[93]B. B. Kadomtsev and V. M. Kontorovich, Isv. Vyssh. Uchebn. Zaved. Radiofiz. **17**, 511 (1974).
[94]M. I. Rabinovich and A. L. Fabrikant, Izv. Vyssh. Uchebn. Zaved. Radiofiz. **19**, 721 (1976).
[95]Yu. I. Kifer, Izv. Akad. Nauk SSSR Ser. Mat. **38**, 1091 (1974).
[96]S. V. Kiyashko and M. I. Rabinovich, Zh. Eksp. Teor. Fiz. **66**, 1626 (1974) [Sov. Phys. JETP **39**, 798 (1974)].
[97]R. V. Flyn and W. M. Manheimer, Phys. Fluids **14**, 2063 (1971).
[98]F. M. Izraĭlev and B. V. Chirikov, Preprint No. 12–73, Institute of Nuclear Physics, Siberian Branch of the USSR Academy of Sciences, Novosibirsk, 1973.
[99]S. Ya. Gertsenshteĭn and V. M. Shmidt, Dokl. Akad. Nauk SSSR **225**, No. 1 (1975) [Sov. Phys. Dokl. **20**, 729 (1975)].
[100]V. I. Yudovich, Asimptotika predel'nykh tsiklov sistemy Lorentsa pri bol'shikh chislakh Rėleya (Asymptotic Behavior of Limit Cycles in the Lorenz System for Large Rayleigh Numbers), Rostov State University, 1977.
[101]J. L. Kaplan and J. A. York, Preturbulence: a Regime Observed in a Fluid Flow Model of Lorenz, Preprint, March 1977.
[102]H. L. Swinney *et al.*, Preprint for Symp. on Turbulent Shear Flows, USA, 1977.
[103]Yu. S. Kachanov, V. V. Kozlov, and V. Ya. Levchenko, Izv. Akad. Nauk SSSR Ser. Mekhanika Zhidkosti i Gaza No. 3, 49 (1977).
[104]C. Normand *et al.*, Rev. Mod. Phys. **49**, 581 (1977).
[105]A. Davey, J. Fluid Mech. **14**, 436 (1962).
[106]A. N. Karashtin and A. G. Sazontov, Izv. Vyssh. Uchebn. Zaved. Radiofiz. **21**, 213 (1978).
[107]M. Henon, Comm. Math. Phys. **50**, 69 (1976).
[108]V. I. Yudovich, in Funktsional'nyĭ analiz i ego primeneniya. Tr. 6–i shkoly po matematicheskomu programmirovaniyu i smezhnym voprosam (in: Functional Analysis and Its Applications. Proc. Sixth School on Mathematical Programming and Adjacent Problems), ANSSSR, M., 1975, p. 44.
[109]L. A. Bunimovich and Ya. G. Sinaĭ, supplement to Ref. 24.
[110]O. I. Bogoyavlenskiĭ, Dokl. Akad. Nauk SSSR **232**, 1289 (1977) [Sov. Phys. Dokl. **22**, 78 (1977)].
[111]A. B. Katok, Ya. G. Sinaĭ, and A. M. Stepin, in Matematicheskiĭ analiz, T. 13 (Itogi nauki i tekhniki) [Mathematical Analysis, Vol. 13 (Reviews of Science and Technology)], VINITI, M., 1975, p. 129.
[112]Smooth Dynamic Systems (Russ. Transl., Mir, M., 1977).

Translated by S. Chomet